Copyright ©

Aus dem Institut für Meereskunde an der Universität Kiel

Currents and stratification in the Belt Sea and the Arkona Basin during 1962—1968

by

Jürgen Kielmann, Wolfgang Krauss and Karl-Heinz Keunecke

Summary: A great number of observations, mainly on temperature and current fluctuations in the Arkona Basin, have been made during the years 1962—1968 (figs. 2 and 4). Corresponding to the wind conditions over the Baltic Sea (mean value about zero, fluctuations of about 5 m sec^{-1}), currents and stratification are extremely variable. The mean currents in fig. 7 are towards NE for the entire eastern part of the Arkona Basin, but the actual flow can have any direction (fig. 32). The current fluctuations are non-Gaussian (fig. 10). The mean stratification in the Arkona Basin underlies also great variations. Temperature fluctuations of 8°C and salinity fluctuations of $3^0/_{00}$ occur within 2 days (fig. 5). In the mean thermocline level we find also in the central part of the Arkona Basin a current towards NE (fig. 9).

The current spectra of the Belt Sea and the Arkona Basin are principally of the same shape, but inertial waves do not occur in the Belt Sea (fig. 13).

The mode decomposition reveals the strongest baroclinity in the period range from approximately 10 h—40 h; at the inertial frequency the major baroclinic mode contains 10 times the energy of the barotropic one (fig. 28). The spectrum of the barotropic mode corresponds to the spectrum of the windstress whereas the spectra of the internal modes correspond to divergence and curl of the stress field (fig. 28).

The strongest signal are the inertial currents. In general their wave length seems to be short; they consist of at least 4 internal modes and the barotropic one (fig. 37).

The Reynolds stress due to inertial waves leads to negative viscosity (fig. 40). The seiches currents are very weak compared to the inertial currents. The oscillations in the Arkona Basin seem to be short-crested and strongly influenced by Bornholm and the Rönne Bank.

Towed thermistor cable records lead to the conclusion that several features of the temperature structure are of quasi-permanent character.

Zusammenfassung: Während der Jahre 1962—1968 wurden im Arkona Becken und in der Beltsee zahlreiche Messungen über Strömungs- und Temperaturschwankungen mit Hilfe von Beobachtungsmasten durchgeführt (Fig. 2 und 4). Entsprechend den Windverhältnissen (Mittelwert nahezu Null, Schwankungen ca. 5 m sec^{-1}) sind Schichtung und Strömung sehr veränderlich. Die mittleren Strömungen setzen im östlichen Teil des Arkona Beckens generell nach NE (Fig. 7), die momentane Strömung kann jedoch jede Richtung annehmen (Fig. 32). Die Stromschwankungen folgen keiner Gaußverteilung (Fig. 10).

Die mittlere Schichtung unterliegt großen Schwankungen. Temperatur und Salzgehaltsänderungen von 8°C bzw. $3^0/_{00}$ treten innerhalb von 2 Tagen auf (Fig. 5). Im Bereich der Temperatursprungschicht findet man auch im zentralen Arkona Becken, abweichend von der sonstigen Stromrichtung, eine Strömung nach NE (Fig. 9).

Die Strömungsspektren in Beltsee und Arkona Becken zeigen den gleichen Verlauf; Trägheitswellen treten jedoch in der Beltsee nicht auf (Fig. 13).

Durch Zerlegung nach Eigenfunktion ergibt sich, daß die stärksten baroklinen Effekte im Periodenbereich von ca. 10—40 h auftreten. Im Bereich der Trägheitswelle beträgt die Energie der 1. baroklinen Eigenfunktion etwa das 10-fache der barotropen (Fig. 28). Das Spektrum des barotropen Anteils entspricht dem Spektrum der tangentialen Schubspannung des Windes, wohingegen die Spektren der baroklinen Anteile sämtlich dem Spektrum von Divergenz und Rotation der Schubspannung entsprechen (Fig. 28).

Das stärkste Signal sind die Trägheitswellen. Ihre Wellenlänge scheint im allgemeinen sehr klein zu sein. Sie setzen sich aus wenigstens 4 internen und der barotropen Welle zusammen (Fig. 37). Der von den Trägheitswellen bewirkte Reynoldsstress führt zu negativen Austauschkoeffizienten (Fig. 40).

Die Seichesströmungen sind schwach im Vergleich zu den Trägheitsströmungen. Die Seiches im Arkona Becken scheinen kurze Kammlängen zu besitzen, was verständlich wird, falls die Schwingungen im Arkona Becken sich aus kreuzenden Wellen zusammensetzen (Umlaufen Bornholms). Schleppkettenmessungen ergeben, daß zahlreiche Inhomogenitäten des Temperaturfeldes quasipermanenten Charakter besitzen.

1. The Belt Sea and the Arkona Basin

The topography of the Baltic Sea can be characterized by a system of basins separated by sills. The westernmost and shallowest one is the Arkona Basin, having a mean depth of 46—48 m. The sea floor rises towards the west to about 20 m, where the Darss sill (18 m) separates the Arkona Basin from the Belt Sea. Detailed maps of the topography have been published by B. SCHULZ (1956).

The Belt Sea covers the area from the Samsö-Belt (sill depth 26 m) to the Darss sill (18 m). Its southern parts are the Kiel Bay, the Bay of Mecklenburg and the Fehmarnbelt, which plays a major rôle for the water exchange between the Kattegat and the Baltic Sea. According to J. P. JACOBSEN (1925), $^4/_5$ of the entire water exchange between these seas occur through the Fehmarnbelt.

The hydrographic conditions in the southern parts of the Belt Sea during summer are characterized by a strong vertical temperature and salinity stratification. According to H. WITTIG (1953), the average salinity at the surface increases from about $10^0/_{00}$ in the east (Gedser) to $17^0/_{00}$ in the north west (Little Belt). Water of low salinity ($10—14^0/_{00}$) flows from the Arkona Basin along the coast of Laaland towards the Great Belt and water of high salinity ($15—18^0/_{00}$) enters the Arkona Basin in the lower layers from the Great Belt towards Fehmarnbelt. The temperature difference between the surface and the bottom water is typically 7—10°C with a thermocline somewhere between 10 and 20 m depth which generally separates the two water masses. Due to the Coriolis force the isohalines are strongly inclined in the Fehmarnbelt (H. WATTENBERG, 1949) where the currents reach maximum values. Towards north, beyond the belts, the less haline surface layer becomes shallower and ends in the Kattegat where the Kattegat water is separated from the Baltic water by a front. Towards east, the Darss sill (18 m) allows only water of generally less than about $20^0/_{00}$ to enter into the Arkona Basin. The position of the Belt Sea front (or several fronts) is highly variable under varying meteorological conditions (H. WATTENBERG, 1949; R. KÄNDLER, 1951). Strong westerly winds of long duration drive the fronts towards east and sometimes beyond the Darss sill. Under strong easterly winds the entire water column can consist of Baltic water in the area from Gedser to Fehmarnbelt flowing towards the Kattegat. Thus, the hydrographic conditions in the Belt Sea are highly variable, depending mainly on the large-scale meteorological conditions. They have been studied mainly at the light vessel Fehmarnbelt (H. WEIDEMANN, 1950; K. WYRTKI, 1953, 1954).

The hydrographic situation in the Arkona Basin has been studied less intensively in former times. The basin is separated towards east from the Baltic proper by the Bornholm island and the Rönne Bank where the bottom rises about 15 m below sea level. This bank with its shallow part, the Adler Grund (6 m), and the shallow areas towards Rügen (about 25 m depth) prevent the haline Kattegat water entering the basin from flowing directly towards east. The only deep connection to the Baltic proper is given by the Bornholm Gatt between Bornholm and Sweden (sill depth 46 m).

The hydrographic conditions in the seas around Bornholm have been subject to several cruises by "Poseidon" during the years 1922—1938 (G. SCHOTT, 1924, B. SCHULZ, 1934, 1956); the observations made, however, have been published only partly. In fig. 1, we display a distribution of salinity 1 m above bottom, based on data of "Posei-

don" obtained during 18. 7.—6. 8. 1938, which shows the spreading of the bottom water towards east. As mentioned above the Rönne Bank and the shallow areas towards Rügen force the haline bottom water which overflows the Darss sill to proceed towards NE. Through Bornholm Gatt it enters the Bornholm basin and spreads SE. Due to the variable overflow of the Darss sill water of different salinity is found in the basins. In the present case more haline water (> $17^0/_{00}$) covers the bottom of the Bornholm Basin whereas the water in the Arcona Basin reaches only $15^0/_{00}$. Several lenses of high salinity can be found near the bottom, depending on the variable inflow.

The hydrographic situation in the Arkona Basin and the Baltic Sea east of Bornholm has been described by G. WÜST (1957) by means of a temperature and salinity section through the deepest areas of the Baltic Sea from Kiel-Helsinki. Under summer conditions a strong thermocline which separates the warm surface layer (about 16°C) from the cold winter water (about 2—4°C) is found in about 20 m depth. The salinity in both water masses is only slightly different. Due to the inflow of Kattegat water the salinity increases strongly near the bottom from about 7—$15^0/_{00}$ in the Arkona and the Bornholm Basin. These mean conditions can be highly disturbed as shown by I. HELA & W. KRAUSS (1959).

A new technique to study the variability in the Baltic Sea by means of moored observation masts has been introduced since 1959 (W. KRAUSS, 1960) which allows to study a broad frequency range of fluctuations. Further information was gained by continuous records of temperature and salinity with depth (G. SIEDLER, 1961, G. KRAUSE 1969) and by towed thermistor chains (K. -H. KEUNECKE, 1972).

The observations carried out by means of observation masts have only partly been published yet. The major contributions have been concerned with:

1. the short periodic fluctuations in the periode range from 0,5—7 hours in the Arkona Basin and the Fehmarnbelt (W. KRAUSS, 1966a),
2. the spectra at Fehmarnbelt obtained during 1962 and 1964 (W. KRAUSS, 1966b),
3. the relationship between the fluctuations in the Arkona Basin and in other areas of the Baltic Sea, mainly at the inertial frequency and in the seiches range (J. KIELMANN, W. KRAUSS & L. MAGAARD, 1969).

In the following sections we review the results on mean conditions and fluctuations obtained during the years 1962—1968.

2. The stations

The measurements during 1962—1968 have been performed with the research vessels "Alkor", "Planet" and "Hermann Wattenberg". The stations carried out in 1962—1965 are given in table 1 and displayed in fig. 2. They concentrate on the western and eastern parts of the area under consideration.

During 1968 it was planned to moore one station (1968—2) for half a year and to add four more stations for a period of four weeks. They were planned to be located along the central axis of the Arkona Basin (WSW—ENE) separated by 3, 6, 12 and 18 nm, allowing horizontal correlations over 3, 6, 9, 12, 18, 21, 24, 27 and 39 nm.

This correlation program failed to be sucessful due to fishery activities in the area which damaged three out of five moorings. The remaining data, however, are still a very useful material. The cruises and the stations are shown in fig. 3. The stations in the Arkona Basin are displayed on a larger scale in fig. 4. Observation masts have been used at stations 1968—2, 1968—3 and 1968—4; at the stations 1968—1 and 1968—5 Geodyne current meters were used. The length of the records obtained is given in table 2a, the positions of which are contained in table 2b.

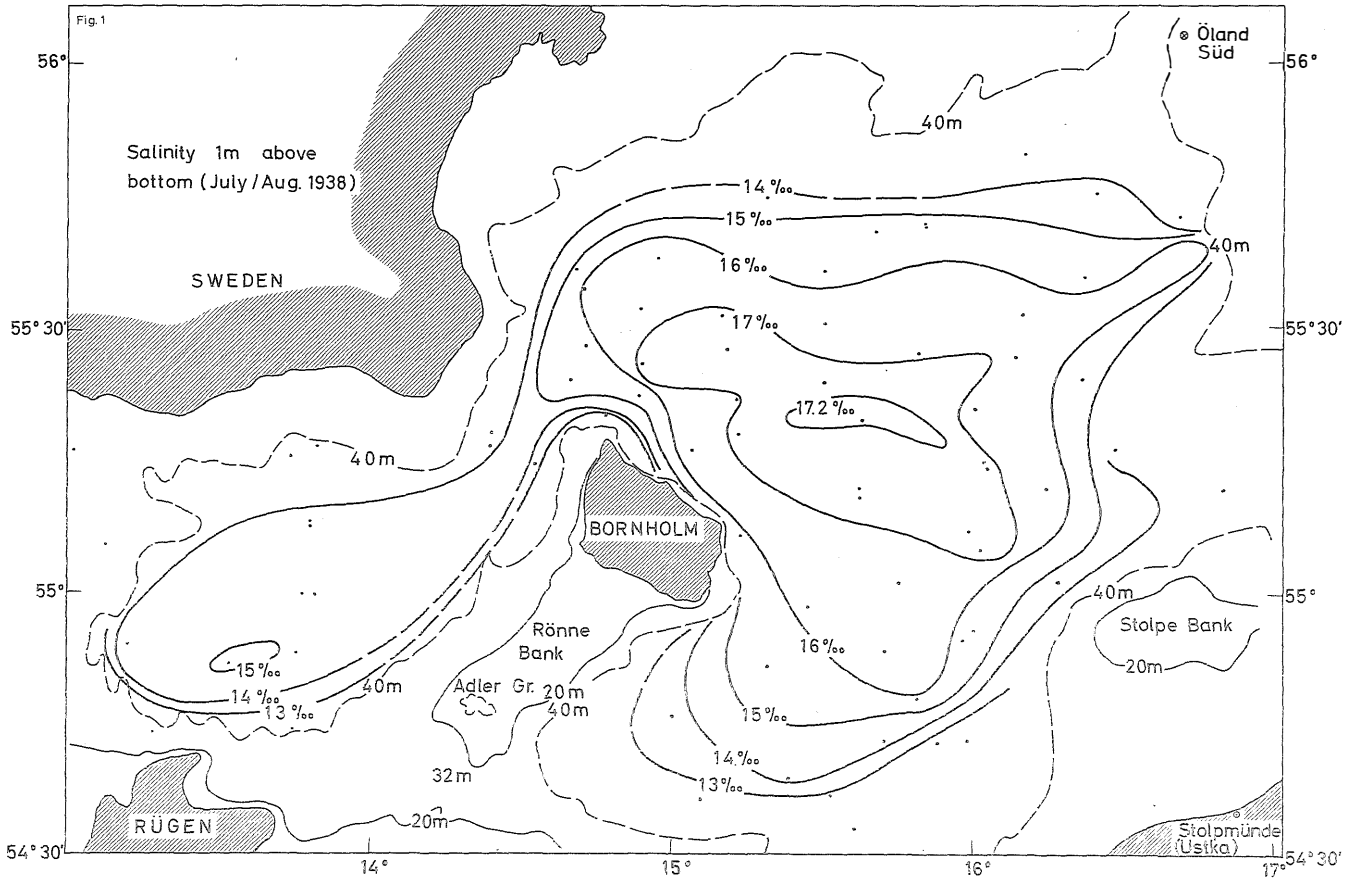

Fig. 1: Salinity distribution 1 m above bottom in July—August 1938

Tafel 1 (zu J. Kielmann, W. Krauß u. K.-H. Keunecke)

Tafel 2 (zu J. Kielmann, W. Krauß u. K.-H. Keunecke)

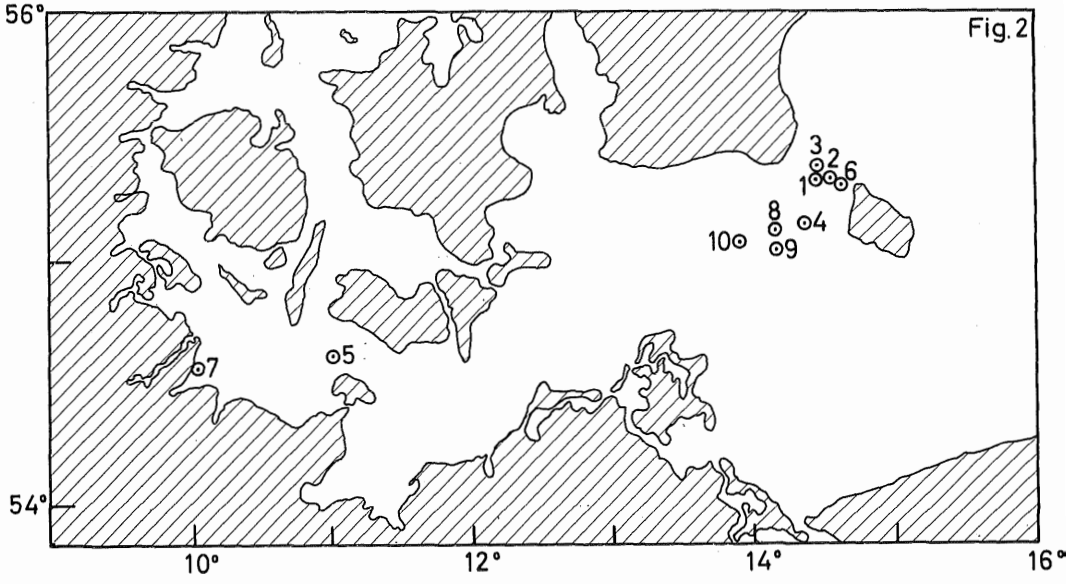

Fig. 2: Position of observation masts during 1962—1965

Table 1: List of stations 1962—1965

No.	Station	φ	λ	depth	sampling Δt	length of record	depth of current meters
1	Bornholm 1962, Mast Süd	55°19,5′N	14°22,2′E	48 m	12 min	21. 8. 7^{50}—30. 8. 14^{00}	9, 19, 23, 29, 33, 43
2	Bornholm 1962, Mast Ost	55°20,6′N	14°25,8′E	51 m	12 min	21. 8. 15^{30}—27. 8. 12^{30}	12, 22, 26, 36, 42, 46
3	Bornholm 1962, Mast Nord	55°21,5′N	14°23,0′E	48 m	12 min	21. 8. 21^{15}—29. 8. 12^{15}	9, 19, 23, 29, 33, 43
4	Bornholm 1963	55°09,6′N	14°17,2′E	44 m	12 min	14. 8. 7^{20}—22. 8. 7^{50}	15, 19, 25, 29, 35, 39
5	Fehmarn 1964	54°36,8′N	10°57,8′E	28 m	1 h	13. 4. 15^{00}— 8. 6. 12^{00}	10, 12, 14, 16, 20, 22, 24, 26
6	Bornholm 1964, Mast II	55°20,2′N	14°29,0′E	54 m	30 min	31. 7. 12^{00}—18. 8. 16^{00}	25, 29, 35, 39, 45, 49
7	Boknis Eck, 1964/65	54°34,9′N	10°06,1′E	25 m	1 h	12.10. 15^{30}—15. 4. 14^{30}	
8	Bornholm 1965, Mast 1	55°05,5′N	14°09,0′E	46 m	2 h	11. 7. 9^{10}—27. 8. 1^{10}	10, 16, 26, 30, 36, 40
9	Bornholm 1965, Mast 2	55°00,0′N	14°09,0′E	45 m	1 h	4. 8. 6^{45}—25. 8. 12^{45}	9, 15, 25, 29, 35, 39
10	Bornholm 1965, Mast 3	55°02,5′N	13°51,0′E	47 m	1 h	4. 8. 6^{10}—25. 8 11^{10}	11, 17, 27, 31, 37, 41

Table 2a: Stations with moored instruments in 1968

Station	Position	Water depth (m)	Period of observation	sampling internal	Number of data poimts
1968—1	φ = 54°57,6′N λ = 13°21,5′E	46,5	4. 6. 10^{31}—15. 6. 03^{50}	20 min	773
1968—2	φ = 53°02,4′N λ = 13°50,6′E	48	15. 5. 12^{10}—16. 10. 04^{10}	2 h	1846
1968—3	φ = 55°04,3′N λ = 14°01,3′E	47,5	4. 6. 14^{00}—16. 6. 22^{00}	2 h	149
1968—4	φ = 55°05,0′N λ = 14°06,0′E	48	4. 6. 15^{45}—24. 7. 19^{45}	2 h	603
1968—5	φ = 55°08,5′N λ = 14°26,0′E	48	4. 6. 18^{02}— 1. 7. 6^{22}	20 min	1910

Table 2b: Anchor stations of "Planet" for continuous T, S measurements

Station	Position	Water depth (m)	Period of observations	sampling interval	Number of profi les
A 1	φ = 55°04,2′N λ = 13°55,8′E	47	17. 7. 21^{00}—20. 7. 06^{00}	30 min	112
A 2	φ = 55°19,3′N λ = 14°41,1′E	48	22. 7. 9^{00}—22. 7. 19^{00}	30 min	20
A 3	φ = 55°03,4′N λ = 13°56,2′E	47	23. 7. 21^{30}—24. 7. 18^{00}	30 min	42

As in earlier years fishery activities in the area conflicted with the program. Stations 1968—1 and 1968—3 could be kept only for a period of about 11 days, station 1968—5 for 3 weeks, station 1968—4 for 7 weeks and station 1968—2 for 5 months. The distribution of instruments is shown in table 2c; the stations 1968—2, 1968—3, 1968—4 have been equipped with current meters and temperature sensors, 1968—1 and 1968—5 with current meters only.

Table 2c

Distribution of instruments

Station	1968—1	1968—2	1968—3	1968—4	1968—5
depths of current records (m)	11	12	11	11	12
	17	18	17	17	18
	27	28	27	27	28
	31	32	31	31	33
	37	38	37	37	38
	41	42	41	41	42
depths of temperature records (m)		14	13	13	
		20	19	19	
		30	29	29	
		34	33	33	
		39	40	39	
		43	44	43	
		46	45	45	

The observation masts have been equipped with a main compass and the current direction was observed relative to the direction of the masts orientation. Due to an instrument failure these compasses did not operate at the positions 1968—3 and 1968—4. For station 1968—4 it was possible to determine the reference direction; station 1968—3 will be omitted due to the shortness of the record.

3. The mean wind field and its fluctuations over the Arkona Basin

The mean wind during a summer period may be inferred from the time 1.5 — 16. 10. 1968. The mean value is very weak over the Baltic Sea. The average wind velocities and air pressures are summarized in table 3 for selected stations shown in fig. 3.

Table 3

Mean values M, mean deviations D for wind velocity components u, v (m sec^{-1}) and air pressure (mb) during 1968

Station	u component		v component		airpressure	
	M	D	M	D	M	D
Fehmarnbelt	— 0.36	6.92	— 0.33	4.32	1 014.8	8.07
Gedser Rev	— 0.72	5.84	— 0.79	4.44	1 014.9	—
Moen	— 0.35	6.98	— 0.25	5.11	—	—
Falsterboe	— 0.85	5.77	— 0.85	4.39	1 013.9	10.54
Dueodde	— 1.23	6.86	+ 0.66	4.23	1 013.6	21.28
Average	— 0.70	6.47	+ 0.31	4.50	1 014.3	13.30

Tafel 3 (zu J. Kielmann, W. Krauß u. K.-H. Keunecke)

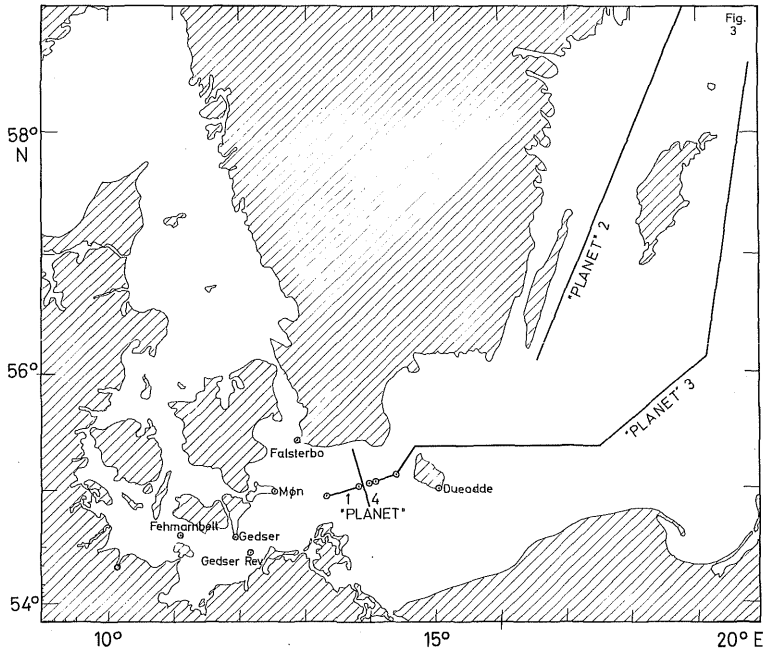

Fig. 3: The cruises 1968 of the research vessels "Alkor" and "Planet"

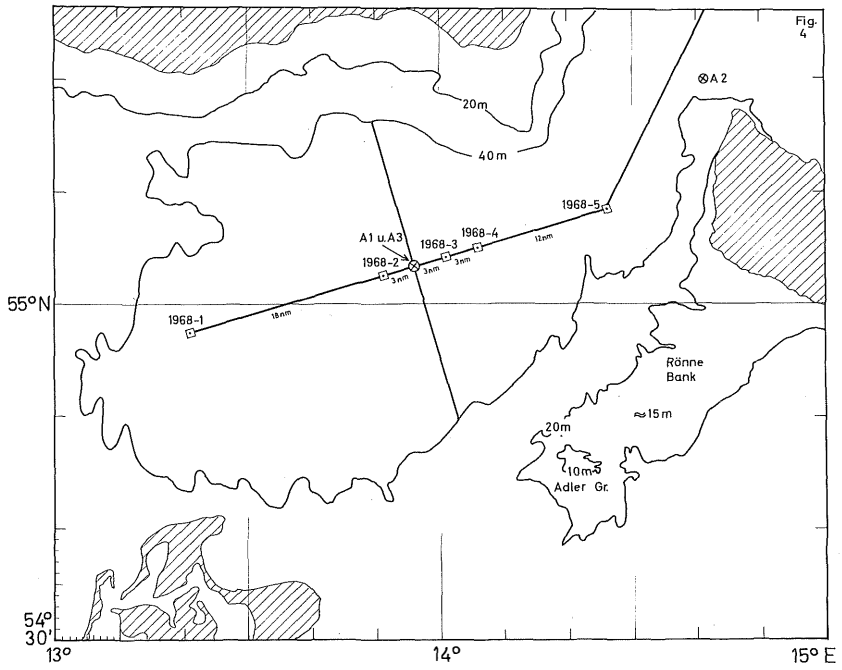

Fig. 4: The anchor station 1968—1 to 1968—5

Tafel 4 (zu J. Kielmann, W. Krauß u. K.-H. Keunecke)

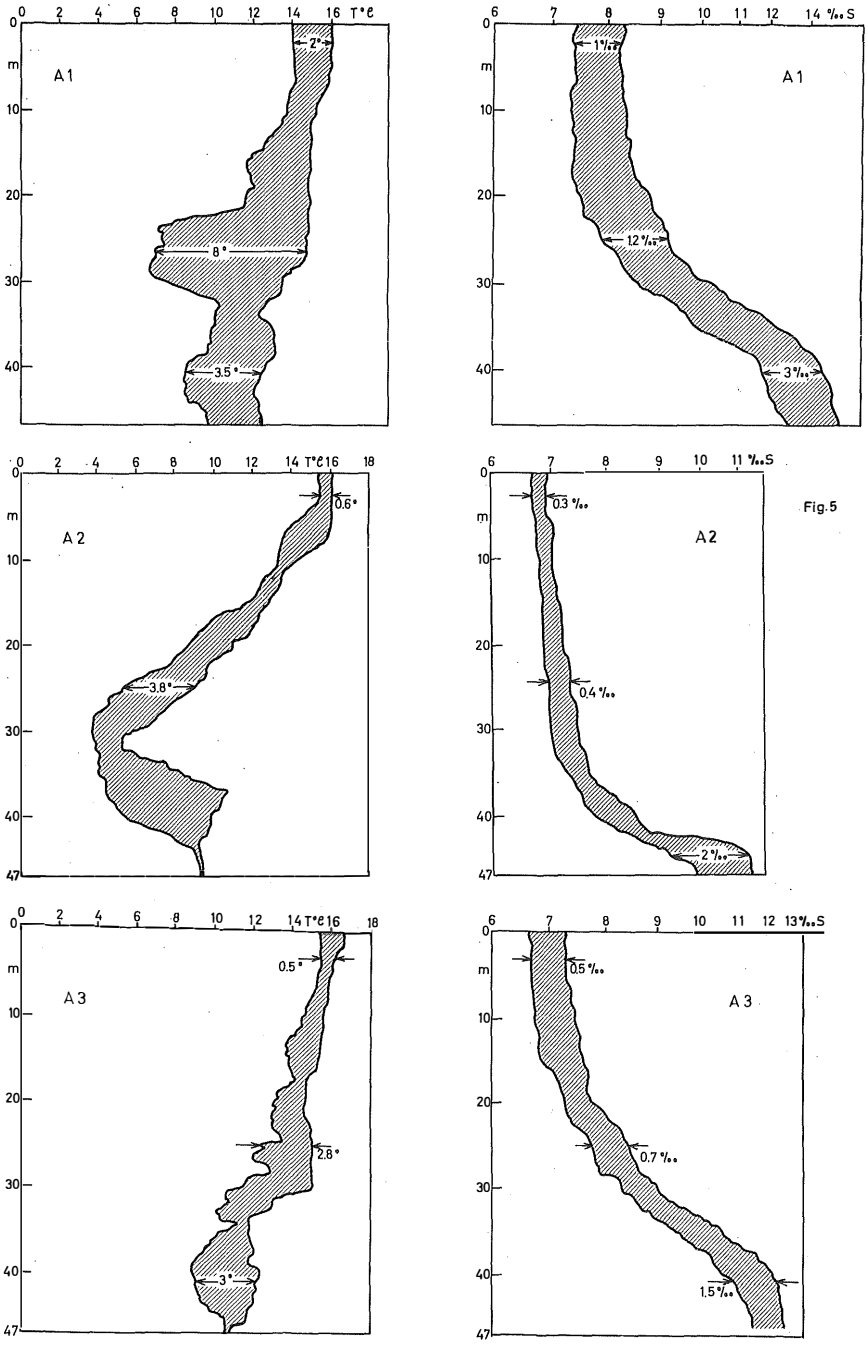

Fig. 5

Fig. 5: Range of temperature and salinity fluctuations during anchor stations A 1, A 2 and A 3, shown in fig. 4

Tafel 5 (zu J. Kielmann, W. Krauß u. K.-H. Keunecke)

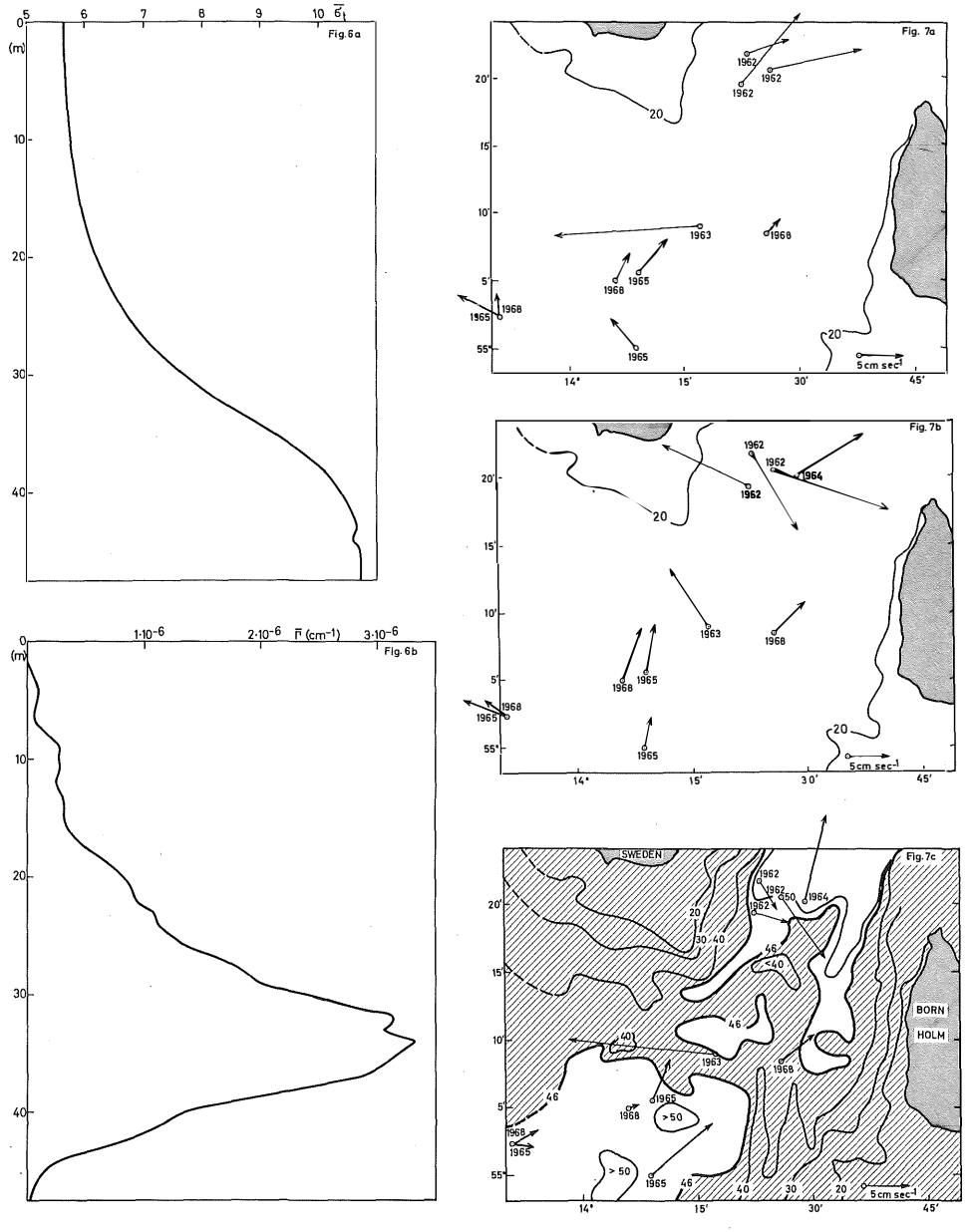

Fig. 6: Mean density ($\overline{\sigma_t}$) and stability distribution Γ at station A 2

Fig. 7a—c: Mean currents in the surface layer 0—20 m (fig. 7a), the cold winter water 20—40 m (fig. 7b) and the bottom water z > 40 m (fig. 7c)

Tafel 6 (zu J. Kielmann, W. Krauß u. K.-H. Keunecke)

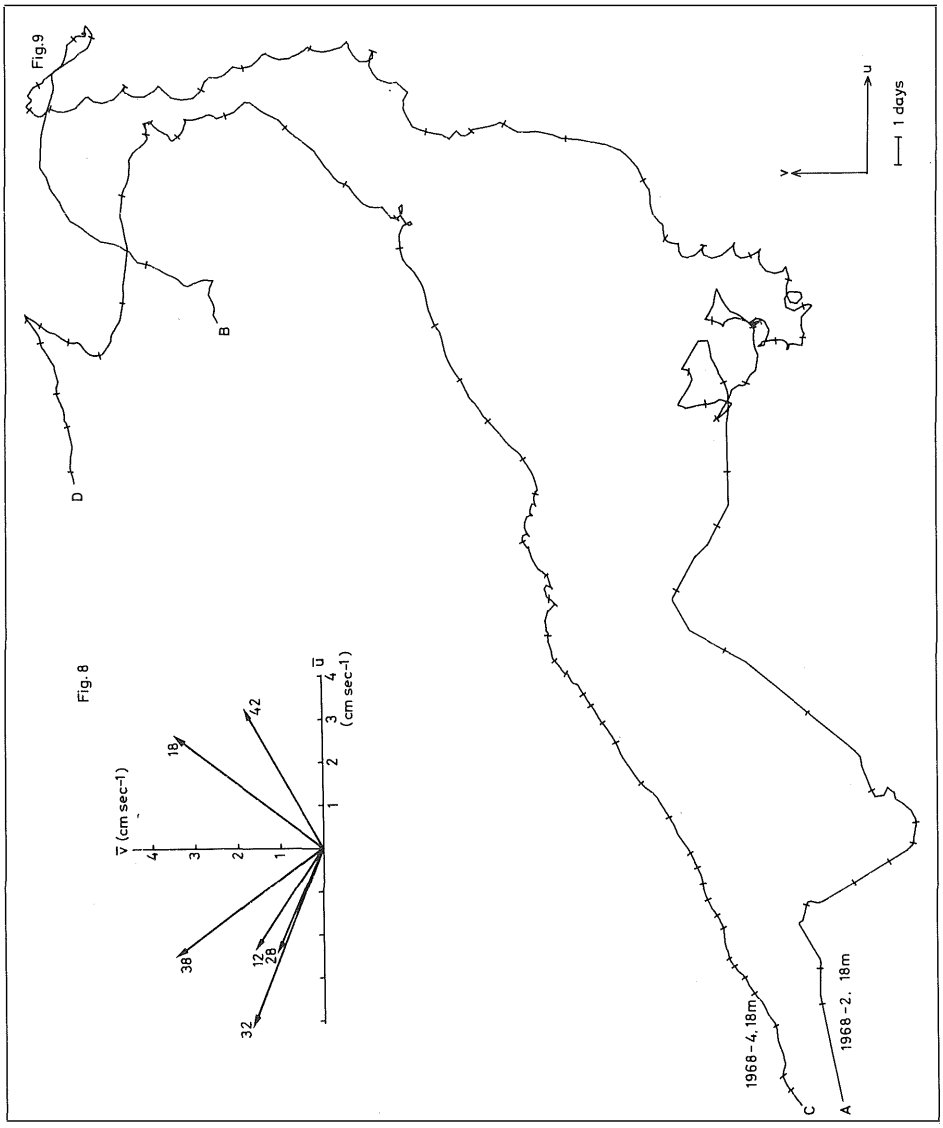

Fig. 8: Mean currents at station 1968—2. The numbers at the arrows indicate the depth (m)

Fig. 9: Progressive vector diagram for 18 m at stations 1968—2 and 1968—4 during the period 4. 6.—24. 7. 1968

The wind field is mainly dominated by fluctuations of an order of magnitude of 5 m sec^{-1} due to meteorological depressions and high pressure cells. The average wind velocity is about $^1/_2$ m sec^{-1} towards NW and, therefore, negligible. In consequence, we find no mean wind produced current system.

4. The vertical temperature and salinity structure in the Arkona Basin

Mean vertical distributions of temperature and salinity can only be determined from a great number of repeated continuous records. Examples are shown in fig. 5, the number of records can be seen from table 2b. The curves show the envelope of the individual records. Typically, three layers are found in the Arkona Basin

a) the warm less haline surface water (about 0—20 m)

b) the cold winter water, having about the same salinity (about 20—40 m)

c) the warmer and haline bottom water (inflow from the Kattegat).

These conditions are best shown at anchor station A 2. The wide range of fluctuations, however, becomes evident from inspection of all the records. Within a period of $2^1/_2$ days, the salinity varies by $3^0/_{00}$ at the bottom and about $1^0/_{00}$ at the surface. The temperature fluctuations are about 2°C at the surface, 8°C within the range of 20—40 m and 3,5°C at the bottom. Within 1 day (A 2, A 3) the fluctuations are less but still remarkable.

For later analysis (eigenfunctions) we need the mean density distribution and the stability $\Gamma = \frac{1}{\bar{\rho}} \frac{d\bar{\rho}}{dz}$. It is obvious from fig. 5 that such mean values can be very misleading with respect to actual events. In fig. 6a and 6b such a mean density and Γ-distribution is displayed for station A 2. The eigenfunction analysis is based on these distributions.

5. The mean currents and their fluctuations in the Arkona Basin

As mentioned above, the mean wind velocity is negligible during summertime. Most of our current measurements extend over a period of less than 6 weeks and, therefore, reflect the prevailing meteorological conditions during that time. In fig. 7a—7c we summarize the mean current conditions based on all records during 1962—1968. Heavy arrows are based on records of more than 14 days. Fig. 7a displays the average currents in the surface layer 0—20 m. In the central parts of the Arkona Basin (lower left corner of fig. 5) the current is towards NW, in the eastern area towards NE. The average velocity is about 5 cm sec^{-1}. The cold winter water (fig. 7b, 20—40 m) moves also towards NW in the central area and towards NE otherwise. The bottom water ($z > 40$ m) (fig. 7c) follows the topography and moves towards NE.

Corresponding to the wind conditions the currents in the surface layer are very weak. The mean velocity increases with depth, indicating that the movements in the cold winter water and the bottom water are not directly produced by the wind but are of thermohaline origin. Mean current velocities of 5—10 cm sec^{-1} in the bottom water are common in the Arkona Basin.

The light arrows in fig. 7 are based on records of less than 14 days. Their direction is highly variable; average velocities of 20 cm sec^{-1} for a period of 8—14 days do occur in all depths, even near the bottom.

The details of the mean current structure in the central Arkona Basin may be seen from station 1968—2, which operated for 5 months (fig. 8). The main current direction between surface and 40 m is towards NW which means an outflow from the Baltic to the Kattegat due to the river surplus. There are, however, two levels with currents towards NE, the 18 m level and the near bottom layer. The flow in the bottom layer towards NE

has been described in fig. 7c already, the currents in the 18 m depth has not been recognized before and cannot easily be understood from linear theories. It is directed 90° towards the right of the surface currents. Its quasi-permanence becomes evident from fig. 9, which shows two progressive vector diagrams for 18 m depth at station 1968—2 (A—B) and 1968—4 (C—D) for the period from 4. 6.—24. 7. 1968. The current occurs in the mean thermocline level between the cold winter water of the Baltic (ranging on the average over $^1/_2$ year from about 20—40 m depth) and the warmer surface layer. In non-rotating systems similar currents (countercurrents) within a thermocline have been observed in laboratory experiments.

As is to be expected from the wind records, strong fluctuations are superposed on the mean current and temperature field. Histograms of these fluctuations are shown in fig. 10a—e for stations 1968—2 and 1968—4. Fig. 10a and d display the histograms of the current components and temperature at station 1968—2 for the entire period of observation. As can be seen from the original records (not displayed) the fluctuations are partly quasi-periodic (inertial waves etc) and partly of stochastic nature. The temperature records additionally contain a longperiodic trend due to the rising temperature during spring. Thus, the data cannot be treated to be uncorrelated. Furthermore, the time series are not stationary in a statistical sense. This also can be seen from the original records, and, additionally, from comparision of fig. 10a with 10b, which shows the histograms of the current components for the shorter period from 4. 6.—4. 7. 1968 only. The distributions show striking differences. Fig. 10c and e display the histograms for station 1968—4. The records of this station are taken at the same time as those used in fig 10b of station 1968—2. Thus, 10b and 10c are directly comparable. Both distributions are significantly different. Therefore, the processes occuring at these two stations, separated by about 9 nm only, must be less correlated. Inhomogeneities in horizontal direction seem to play a dominant rôle. Even in vertical direction marked differences occur as has been proven by a χ^2-test. Finally, it may be noticed that the histograms are, in general, not Gaussian. Due to the large fluctuations a Gaussian distribution would be flat compared to the observed ones. We come to the conclusion that the fluctuations are dominated by quasiperiodic phenomena (mainly inertial waves) which are either small-scale phenomena (locally created) or which are strongly distorted horizontally by superimposed stochastic processes or spatial inhomogeneities.

The quasiperiodic nature of the dominant processes becomes evident from inspection of fig. 11 which displays autocorrelation functions of the current components of station 1968—2. The autocorrelation functions decrease rapidly for time intervals of a few days and remain periodic (inertial period) afterwards.

The dominant rôle of the inertial waves is also evident from the mean kinetic energy spectrum of station 1968—2 (fig. 12). The mean spectrum $(u^2 + v^2)/2$ is obtained by averaging over all depths. The general slope of the spectrum is due to the wind spectrum (next section), the minor peaks have been interpreted as seiches and their non-linear interaction with the 120^h — wave (W. KRAUSS, 1973). The dominant peak reveals inertial waves.

6. The velocity spectra in the Belt Sea and the Arkona Basin

The main differences between the Belt Sea and the Arkona Basin in the fluctuations of the currents may be seen from fig. 13 which displays the amplitude spectra of the current components at Boknis Eck (a, b), northwest of Fehmarn (c, d), in the Arkona Basin (e, j) and in the Bornholm Gatt (k, l). As will be described in the next section, the general slope of the spectra corresponds to that of the wind spectra. The most striking

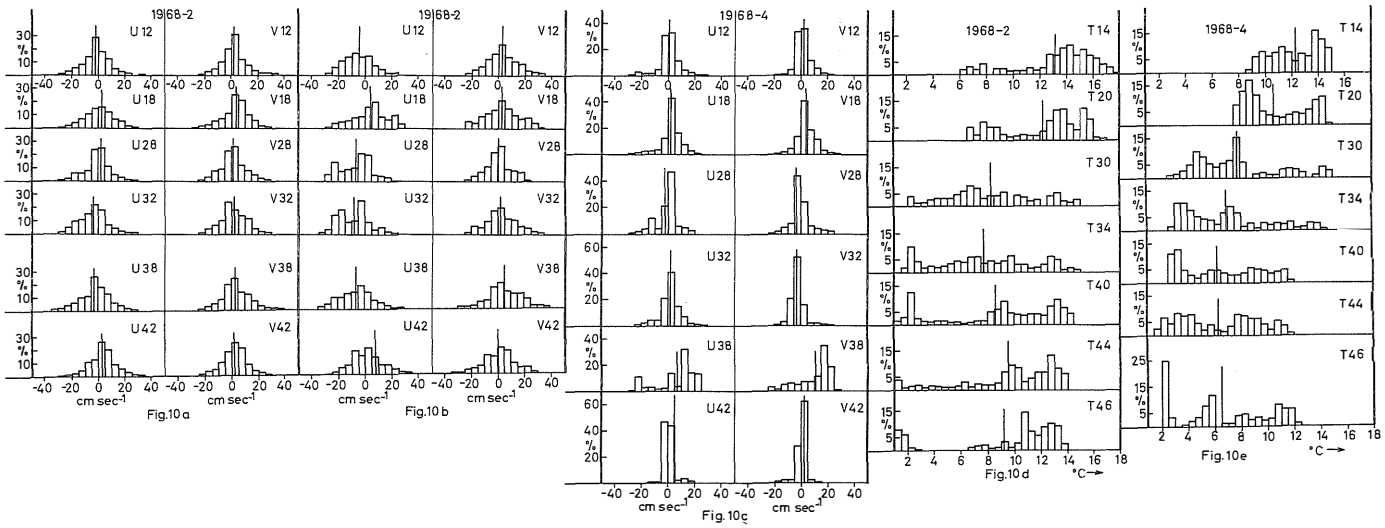

Fig. 10: Histograms of velocity components and temperature fluctuations

a) velocity components at station 1968—2, total period
b) the same for the period 4. 6.—24. 7. 1968
c) the same at station 1968—4
d) temperature at station 1968—2
e) temperature at station 1968—4

Tafel 7 (zu J. Kielmann, W. Krauß u. K.-H. Keunecke)

Tafel 8 (zu J. Kielmann, W. Krauß u. K.-H. Keunecke)

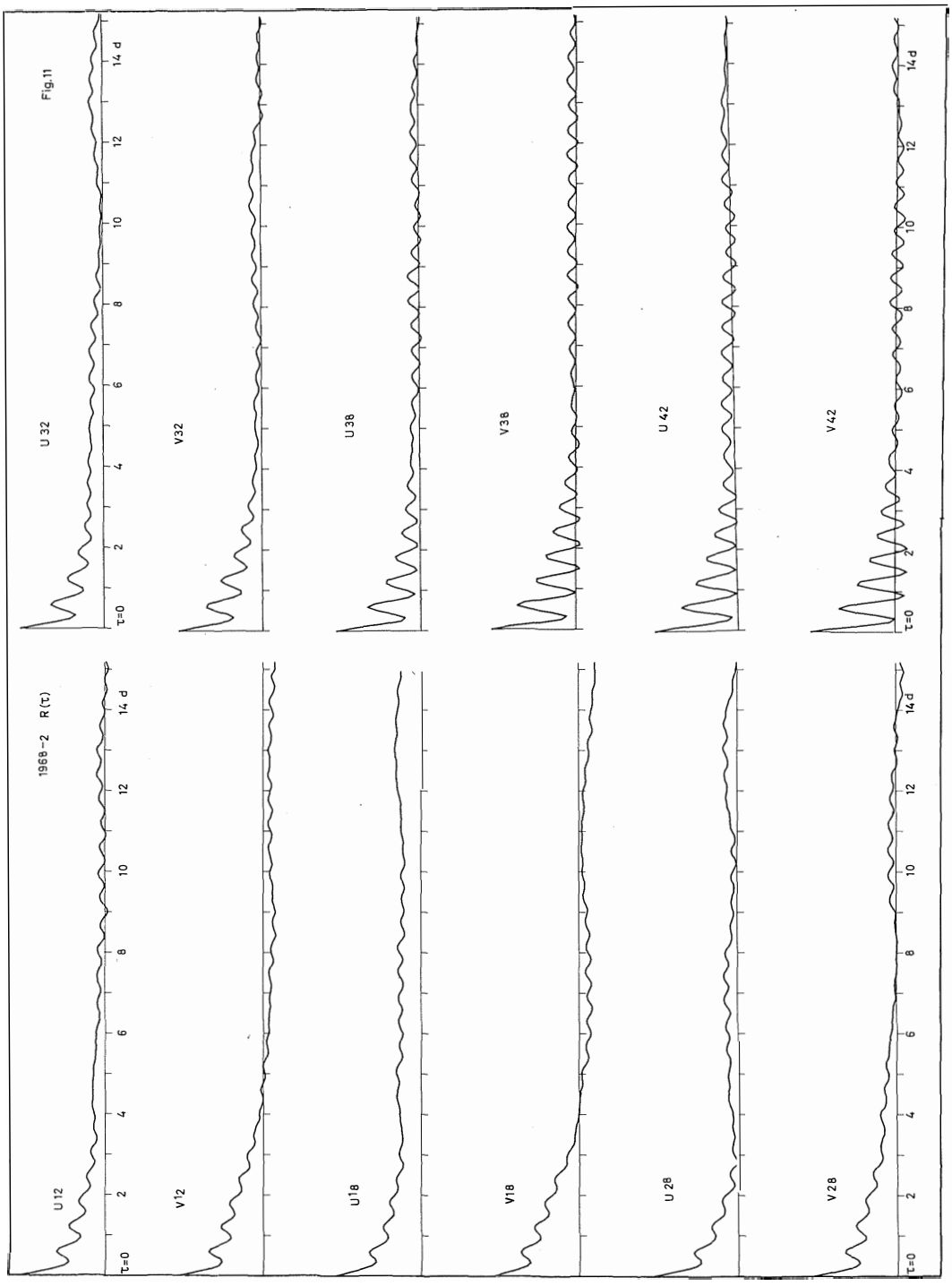

Fig. 11: Autocorrelation functions of the velocity components at station 1968—2

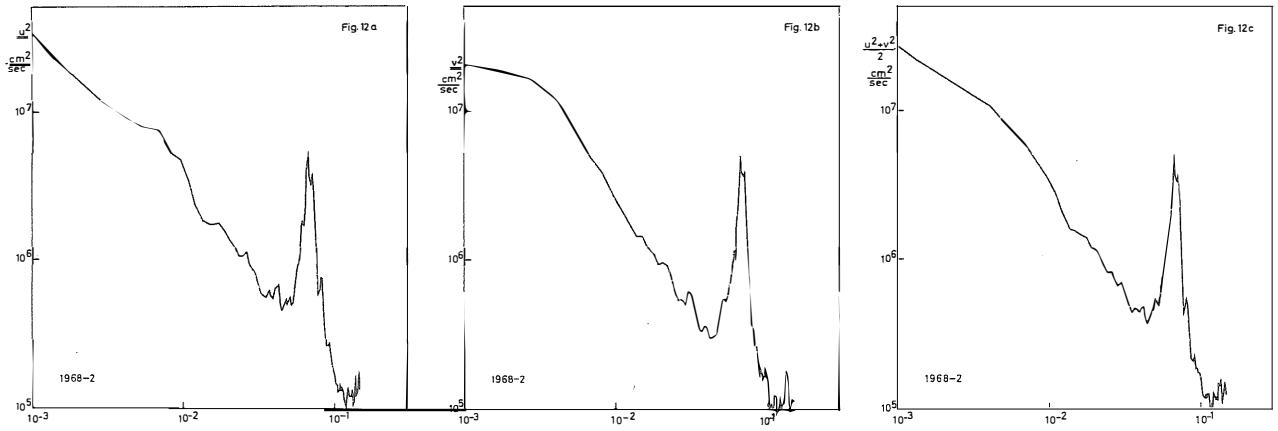

Fig. 12: Vertically averaged energy spectra at station 1968—2; a) u^2, b) v^2, c) $(u^2 + v^2)/2$

Legend for figure 13 see next page

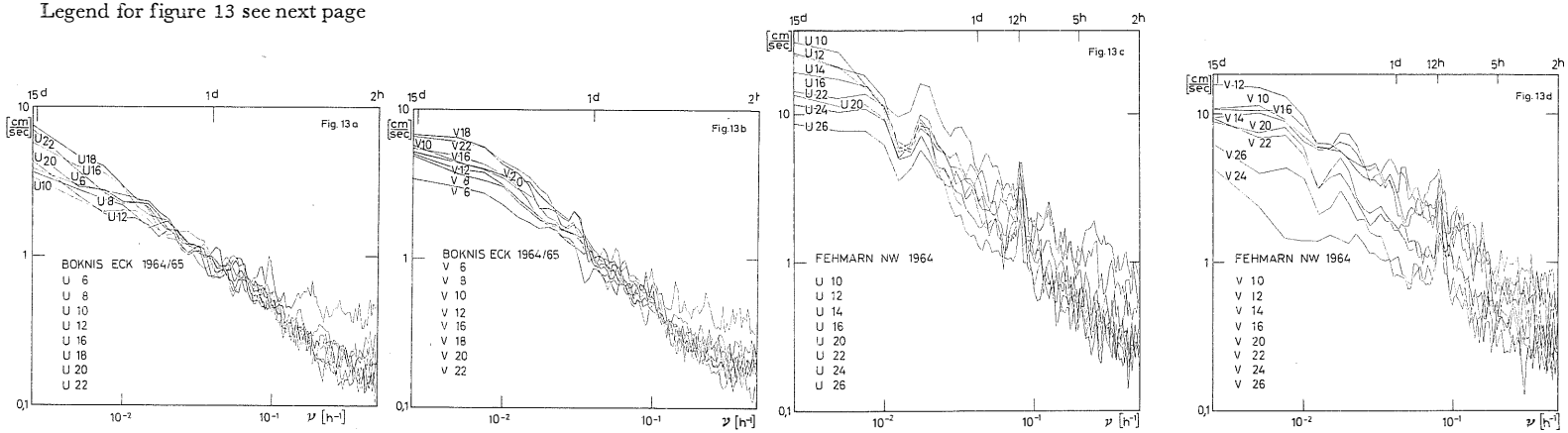

Fig. 13: Amplitude spectra of current velocities at Boknis Eck (a, b), northwest of Fehmarn (c, d), in the Arkona Basin (e, j) and in the Bornholm Gatt (k, l)

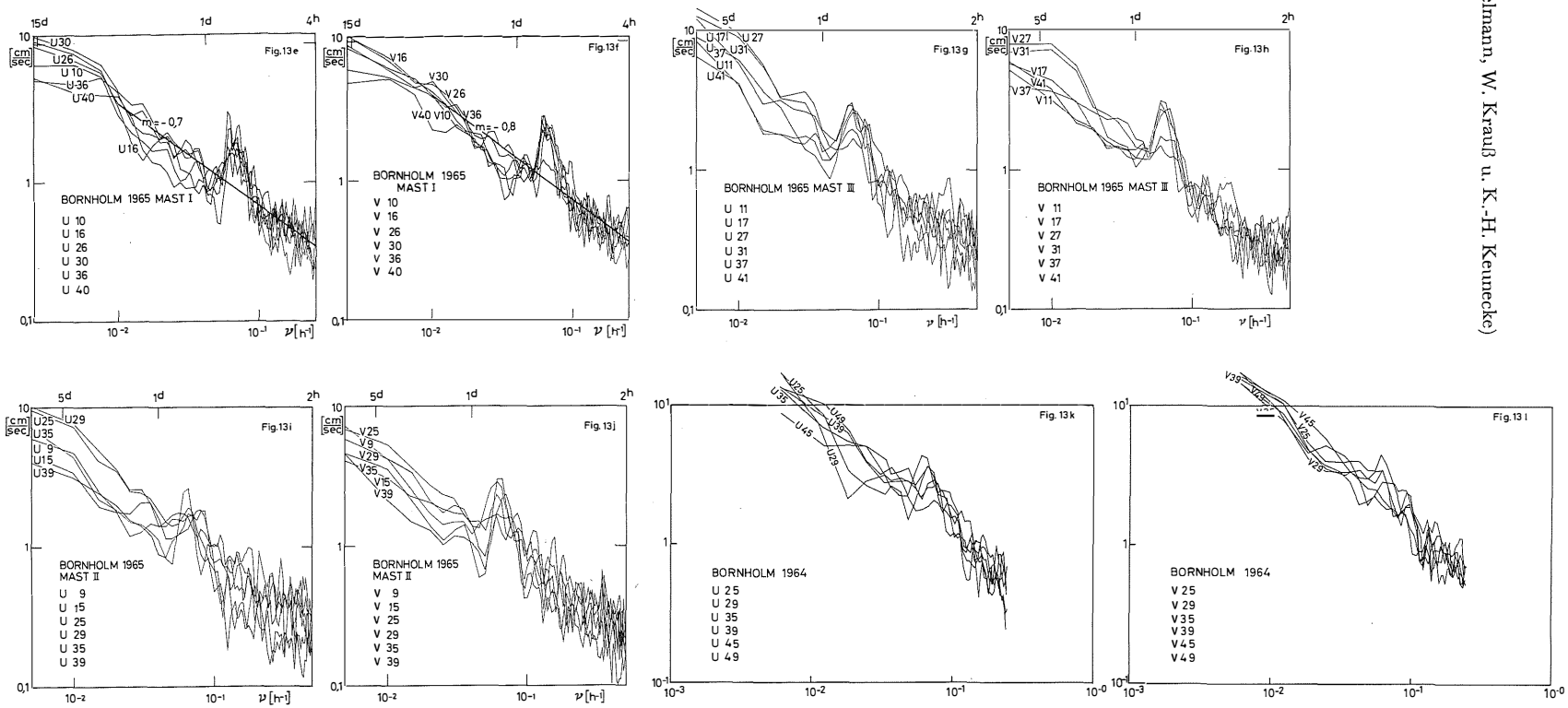

Tafel 11 (zu J. Kielmann, W. Krauß u. K.-H. Keunecke)

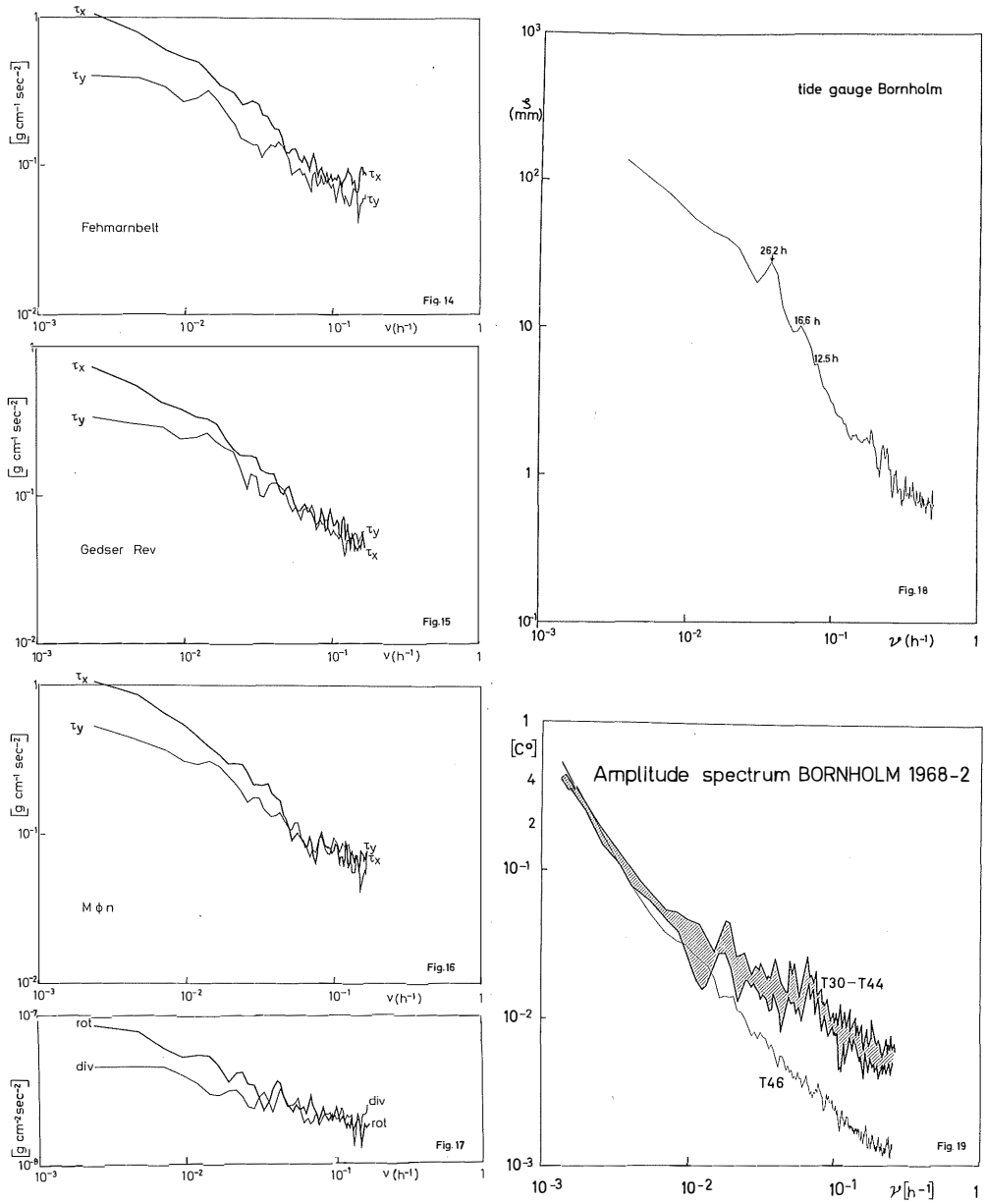

Fig. 14: Spectra of the components of the tangential stress at Fehmarnbelt

Fig. 15: Spectra of the components of the tangential stress at Gedser Rev

Fig. 16: Spectra of the components of the tangential stress at Moen

Fig. 17: Spectra of $\mathrm{div}\,\overset{(\rightarrow)}{\tau}$ and $\mathrm{rot}\,\overset{(\rightarrow)}{\tau}$

Fig. 18: Sea level spectrum at Bornholm island

Fig. 19: Temperature spectrum 2 m above the bottom (46 m) and in the interior of the water body

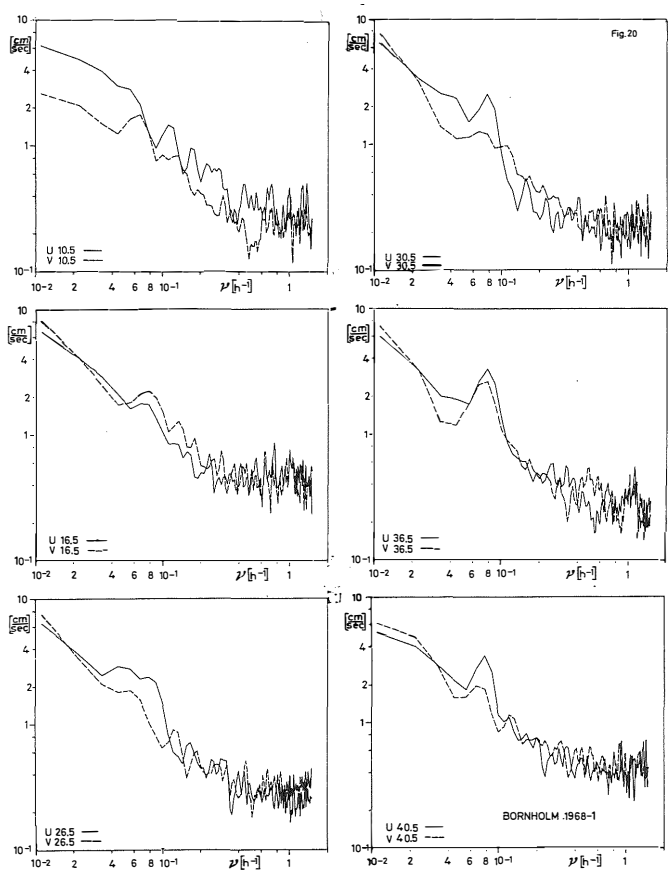

Fig. 20: Amplitude spectra of the current components at station 1968—1

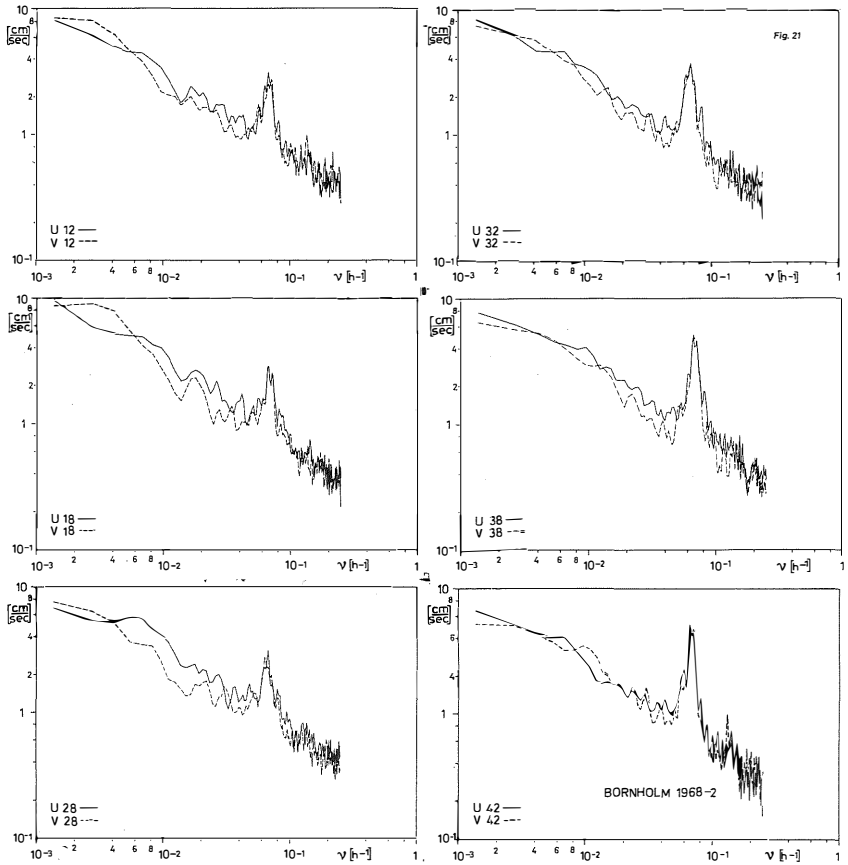

Fig. 21: Amplitude spectra of the current components at station 1968—2

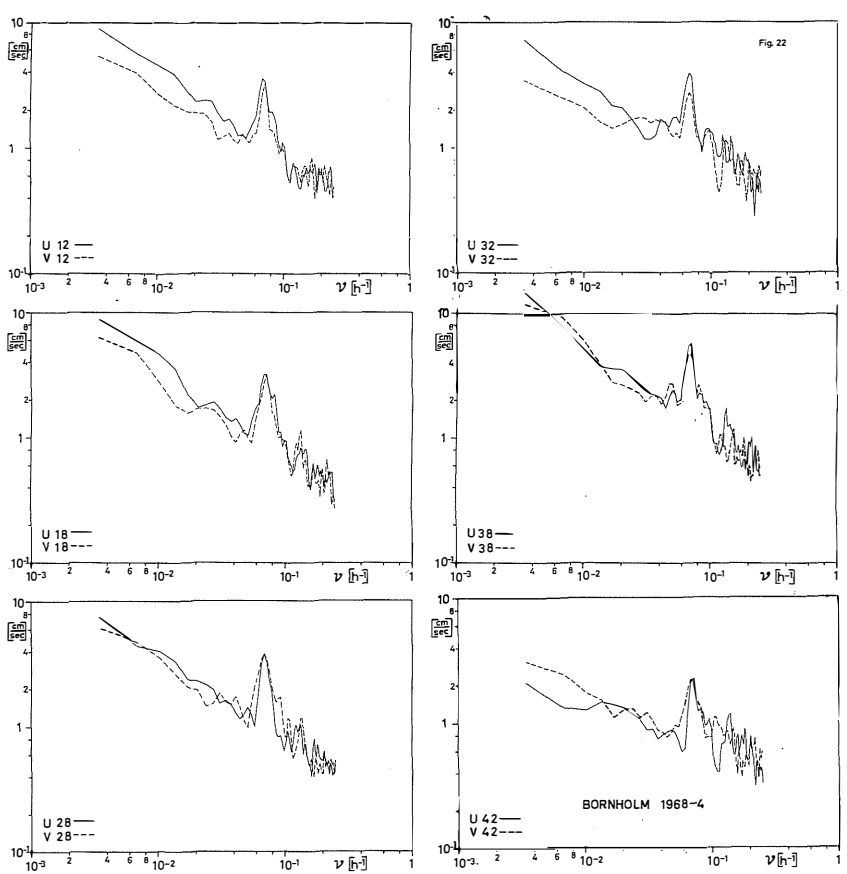

Fig. 22: Amplitude spectra of the current components at station 1968—4

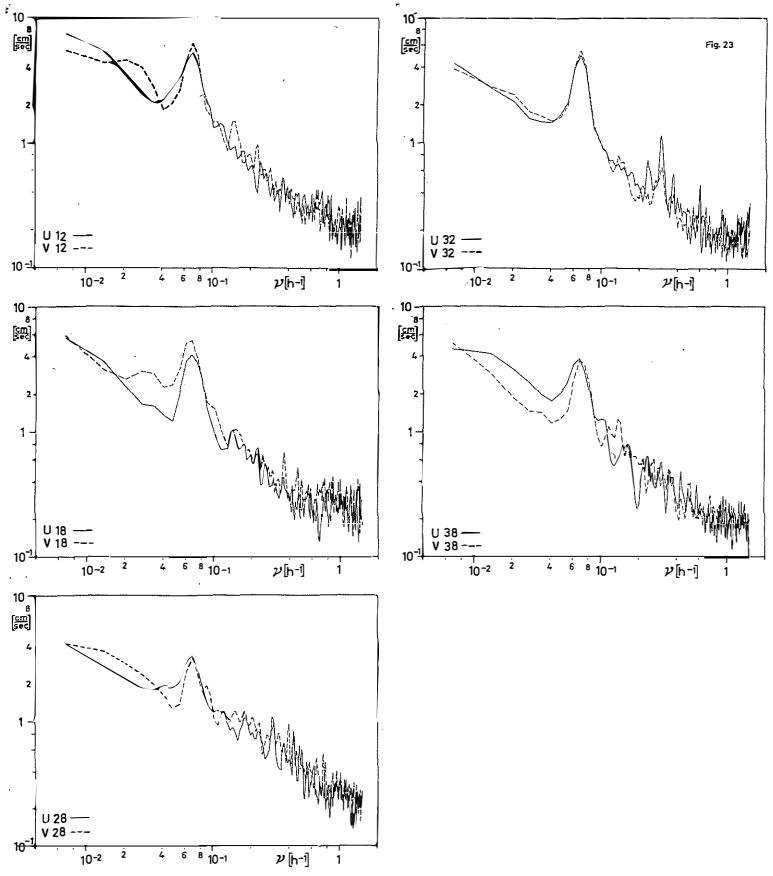

Fig. 23: Amplitude spectra of the current components at station 1968—5

Tafel 14 (zu J. Kielmann, W. Krauß u. K.-H. Keunecke)

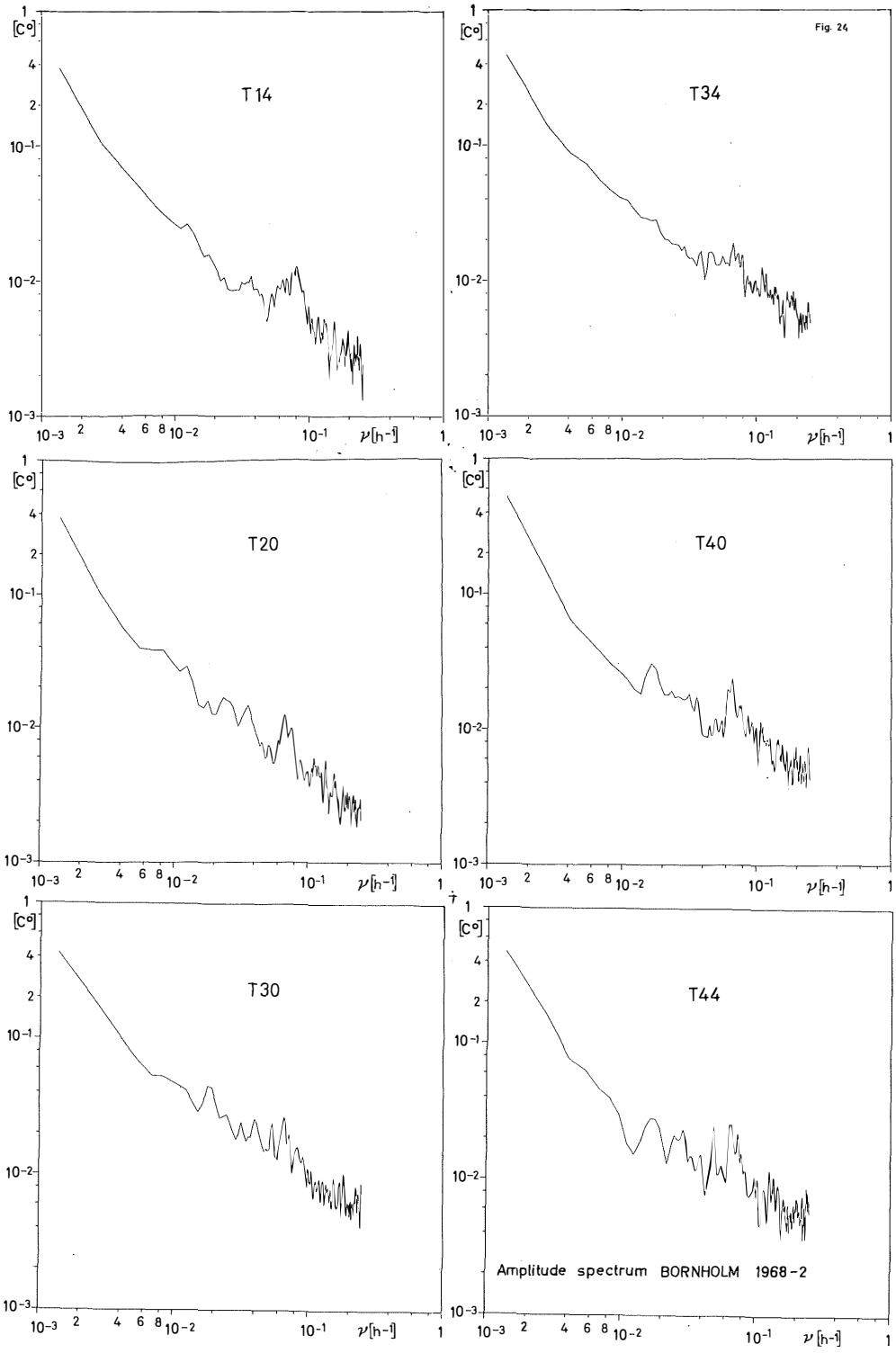

Fig. 24: Amplitude spectra of temperature records at station 1968—2

difference between the spectra in the Belt Sea and the Arkona Basin is the occurence of inertial waves in the Arkona Basin (peak at about 14 hours). They do not occur in the Belt Sea which seems to be too small for their occurence.

7. The amplitude spectra 1968

By means of power spectra analysis the energy distribution as a function of frequency (hours^{-1}) has been computed for some meteorological stations and for the current and temperature records of 1968. They are displayed in figs. 14—23 as amplitude spectra.

Figs. 14 and 15 show spectra of the tangential stress of the wind at the light vessels Fehmarnbelt and Gedser Rev. Fig. 16 is the spectrum of the station Moen. The stress spectra have been computed according to $\vec{\tau} = \rho c \mid \mathfrak{v} \mid \mathfrak{v}$, using $c = 1{,}2 \cdot 10^{-3}$. The spectra decrease with increasing frequency ν approximately according to $\nu^{-0.7}$ in the range $10^{-2} < \nu < 5 \cdot 10^{-1}(h^{-1})$ and according to $\nu^{-0.3}$ for $\nu < 10^{-2}(h^{-1})$. The eastcomponent of the stress, $\tau^{(x)}$, is stronger than the north component, $\tau^{(y)}$, due to the prevailing southwesterly winds (Data: May—October 1968). The wind is the main driving force for the currents in the Ekman layer. The fluctuations in deeper layers should be additionally produced by the curl and the divergence of the wind field (M. Tomczak, 1966, 1967; W. Krauss, 1972). Informations about curl and divergence are difficult to obtain from standard observations. The stations Fehmarnbelt and Gedser Rev are separated by approximately 69 km, Moen is located 60 km from Gedser Rev, lying on a line perpendicular to the connection between Fehmarnbelt and Gedser Rev. We, therefore, tried to compute also the spectra of the curl (rot) and the divergence (div) of the tangential stress from the same records (about 6 months) used in figs. 14—16. The spectra are shown in fig. 17. Compared to the stress spectra the spectra of rot $\vec{\tau}$ and div $\vec{\tau}$ are rather flat; they decrease according to $\nu^{-0.3}$. The air pressure (not reproduced) obeys a law proportional to $\nu^{-1.6}$. The sea level spectra of the Baltic Sea for long records (1 year) (L. Magaard& W. Krauss, 1966) have generally a shape which can be approximated by $\nu^{-1.1}$ in the range $10^{-2} < \nu < 5 \cdot 10^{-1}\,(h^{-1})$. For the present purpose we installed a tide gauge at Bornholm (Hammershavn) for the time from 5.6. 12^h—23. 7. 11^h 1968. The spectrum is shown in fig. 18. Besides a general slope according to $\nu^{-1.3}$ peaks occur at the seiches periods $26{,}2^h$ and $16{,}6^h$, being the first and second harmonic of the system Western Baltic — Gulf of Finland. The temperature spectrum 2 m above the bottom (T 46) of the $^1/_2$ year record at station 1968—2 is shown in fig. 19. It falls off like the sea level spectra (of long records) according to $\nu^{-1.1}$, giving some indication that the shape of this spectrum is governed by the same processes as the spectrum of the sea level fluctuations. In the interior of the water body (30—44 m as examples) the spectral level is raised considerably in the range $10^{-2} < \nu < 10^{-1}(h^{-1})$, probably due to internalmodes. There is, however, no cut-off at the inertial frequency. The current spectra of stations 1968—1, 1968—2, 1968—4 and 1968—5 are displayed in figs. 20—23 (u 12, v 12 = u and v component in 12 m depth). Depending on the lengths of the records of the different stations and of the sampling interval shown in table 1 the resolution and bandwidth is different for different stations.

The general shape of the spectra is the same as that of the tangential stress of the wind ($\nu^{-0.7}$) indicating the strong relation between wind stress and currents observed. The peak at the inertial frequency is a common phenomena of all stations and all depths.

The temperature spectra of station 1968—2 are shown in fig. 24. As mentioned above the energy level is raised for frequencies above $\nu \approx 10^{-2}$ (h^{-1}).

The following laws can be derived for the spectra:

Wind velocity	$U \sim \nu^{-0.7}$	Current velocity	$u \sim \nu^{-0.7}$
Tangential stress	$\tau \sim \nu^{-0.7}$	Sea level	$\zeta \sim \nu^{-1.1}$
Air pressure	$P_L \sim \nu^{-1.6}$	Temperature near the bottom	$T_B \sim \nu^{-1.1}$
Divergence and curl of the wind stress	$\sim \nu^{-0.3}$	Temperature in the interior	$T \sim \nu^{-0.7}$

8. The energy distribution as function of frequency and depth

The records of 1963 and 1965 Mast 1 have been used to plot the energy distribution as a function of frequency and depth (fig. 25a and b). From fig. 25a we conclude that the period range from 10 h — 40 h (seiches range and inertial period band) is the range of highest variability. The energy in this range is strongly dependent on frequency and depth. For periods longer than about 50 hours the energy becomes nearly independent on depth which means that the Baltic responds mainly barotropically for low frequencies. Thus, the stratification may be neglected in a first approximation for long-periodic processes (G. WALIN, 1972). For higher frequencies (periods less than 10 hours), the energy decreases rapidly with increasing frequencies. This is displayed on a larger scale in fig. 25b for periods less than 10 hours.

9. The energy distribution in the seiches range and at the inertial frequency

The range between 10 hours and 40 hours thus remains as that range in which the processes are dominated by baroclinic effects and in which the energy level is comparable to the longperiodic one.

In fig. 26a—g we display energy distributions for this range. All have in common that the highest energy occurs close to the inertial frequency. Often we find at this frequency an energy maximum in the surface layer, a minimum in the thermocline depth (about 20 m) and at least a second maximum in the deeper layers. This can be interpreted by the mechanism proposed by W. KRAUSS (1972): the inertial waves in the surface layer are due to the direct influence of the variable wind whereas the maximum below the thermocline stems from curl or divergence of the wind field. Besides the energy concentration close to the inertial frequency a secondary maximum below the thermocline is very common somewhere in the seiches range. For comparision, the theoretically obtained seiches periods (W. KRAUSS & L. MAGAARD, 1962) are indicated at the top of each figure. Generally, the maxima do not occur at any of the theoretical eigenperiods.

The 1962-stations (figs. 26a—c) are separated by 2 nm only, the 1965 stations by 5 nm (station 2 and 3) and 10 nm (station 1 and 2, 1 and 3). Even over these short distances remarkable differences occur.

10. The mode structure

For barotropic oscillations in narrow elongated basins it is known that the Coriolis force is of secondary importance (A. DEFANT, 1960; D. B. RAO, 1966). Free baroclinic modes, however, are strongly dependent on f. They either exist as Kelvin waves, limited to a narrow strip along the coast or are bounded by the frequency limits N and f. We believe that the observed fluctuations (besides inertial currents) are mainly forced ones.

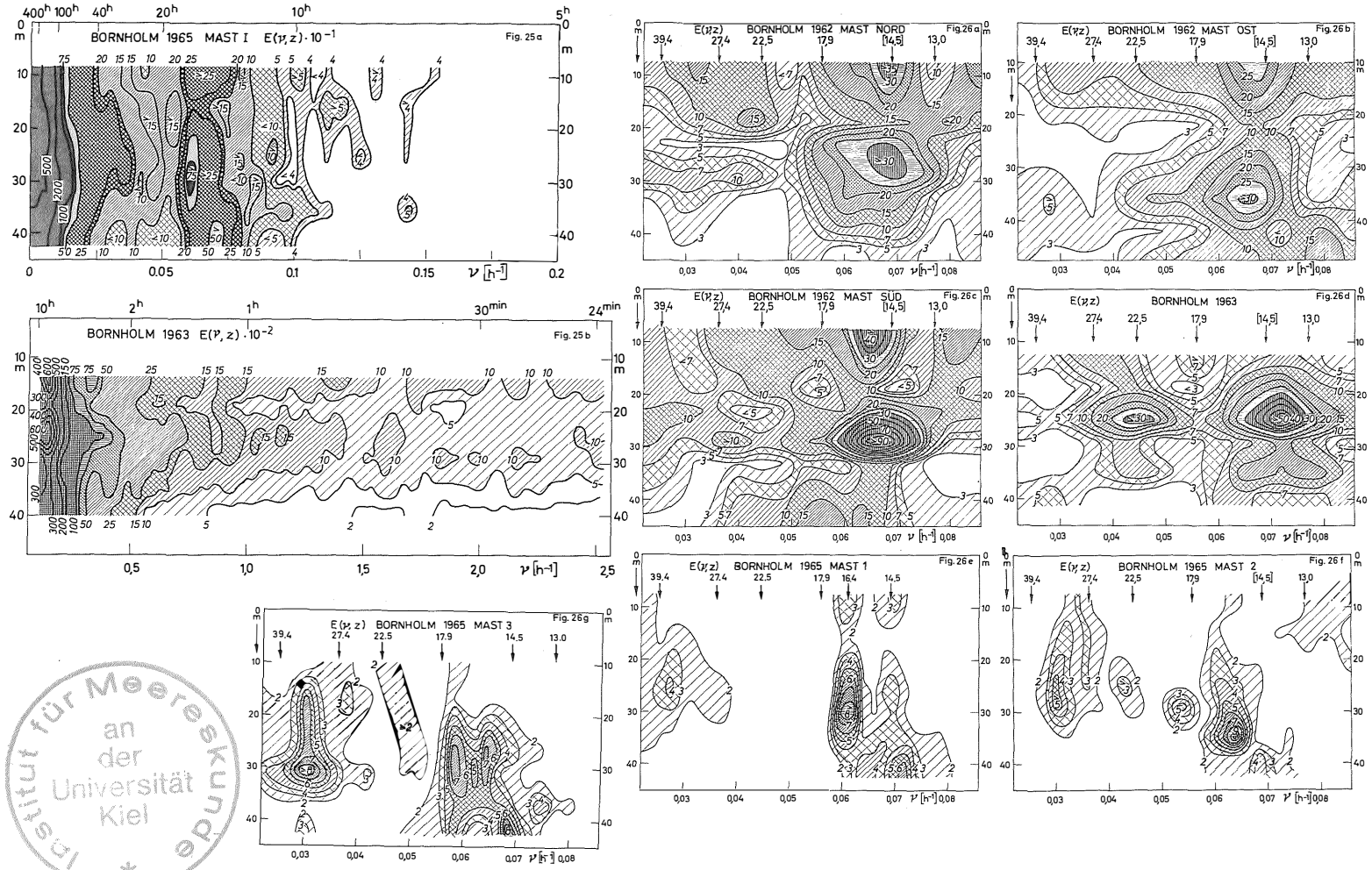

Fig. 25a, b: Kinetic energy as function of frequency and depth

Fig. 26a—g: Kinetic energy as function of frequency and depth in the period range 10—40 hours

Tafel 16 (zu J. Kielmann, W. Krauß u. K.-H. Keunecke)

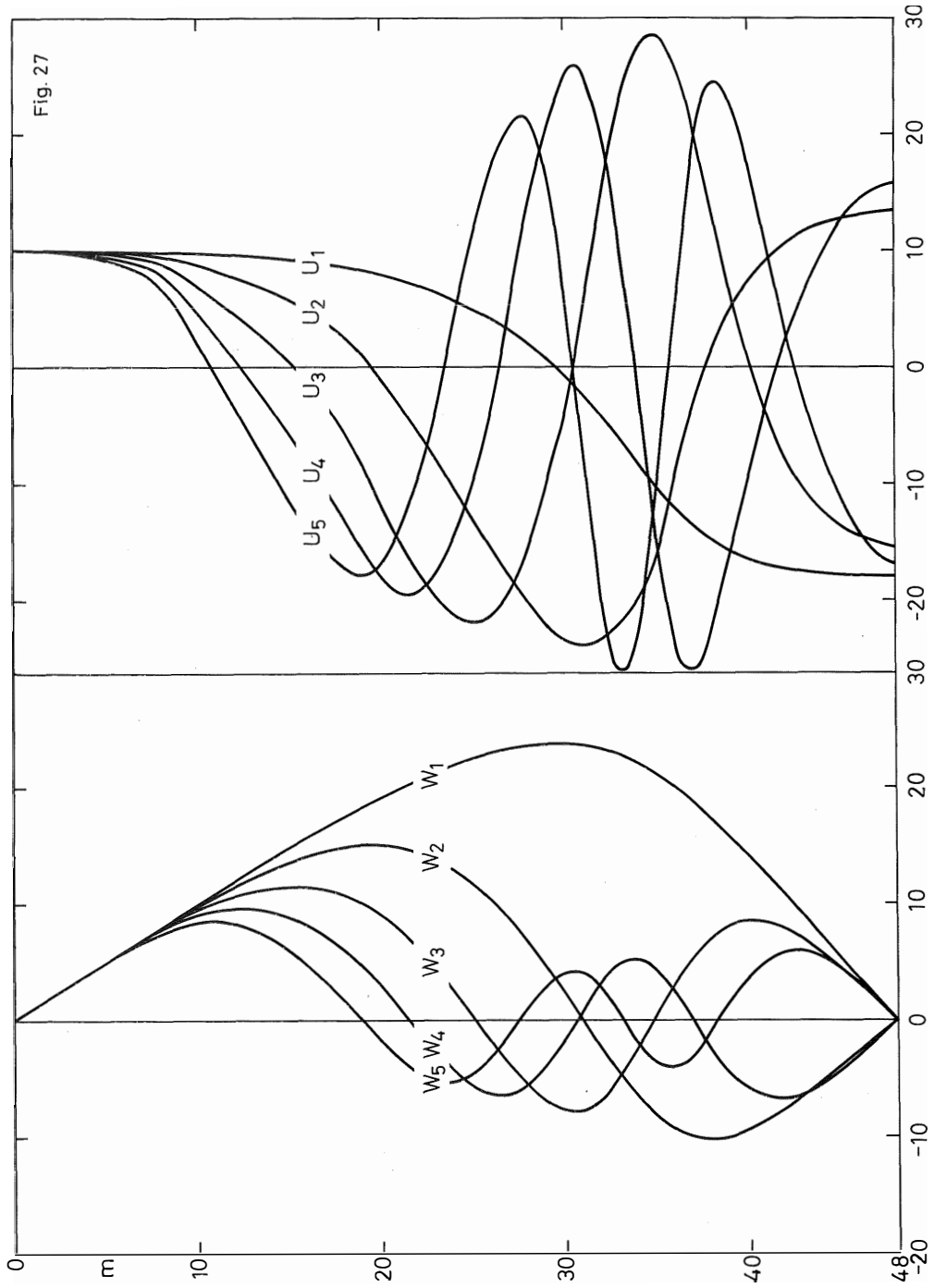

Fig. 27: 1.—4. modes at station 1968—2
(left: vertical velocity w, right: horizontal velocity component u)

The main forcing function for ocean currents is the wind which produces surface currents and a well mixed layer near the surface (Ekman layer). Ekman suction occurs at its lower boundary. This Ekman suction is the main driving force for the deeper (stratified) layers. As shown in the appendix these forced motions in the deep layers can be formally decomposed into the system of modes of the entire water column. There is no restriction with respect to frequency. The only condition to be fullfilled for the decomposition is that the measurements are taken outside the viscous surface layer.

In the Arkona Basin the Ekman layer should have a depth of about 10—15 m. Our measurements generally cover the layers deeper than 12 m .Therefore, only the velocities at 12 m could be influenced by a small Ekman current which decreases exponentially from surface to 12 m.

The mode structure of the half-year records of station 1968—2 has been computed by the following procedure:

1. The time series u (z_i) and v (z_i) have been filtered for the frequency bands shown in table 4.
2. At each time step the filtered series have been decomposed into the 0^{th}, 1^{st}, 2^{nd}, 3^{rd} and 4^{th} mode A_n (t) φ_n by the method of least squares (W. KRAUSS, 1966c p. 205ff). The eigenfunctions are based on the density distribution of fig 6 and are shown in fig. 27.
3. From the amplitude distribution A_n (t) the variance

$$s^2_n = \frac{1}{M}\sum_{m=1}^{M} (A_n(t_m) - a_n)^2 \text{ is computed} \qquad a_n = \frac{1}{M}\sum_{m=1}^{M} A_n(t_m) \quad).$$

4. In order to interprete the variance as an energy measure the s_n^2 are divided by the frequency band of the filter width forwhichthis energy is representative $E_n = s^2_n/\triangle\nu$.

Table 4

Frequency bands used for filtering

Central Frequency (h—1)	Period (h)	Filter limits (h)	bandwidth (h—1)
$1 \cdot 10^{-3}$	1000	1050 —666	10^{-3}
2	500	666 —400	,,
3	330	400 —285	,,
4	250	285 —222	,,
5	200	222 —181	,,
6	166	181 —154	,,
7	143	154 —133	,,
8	125	133 —117	,,
9	111	117 —105	,,
$1 \cdot 10^{-2}$	100	105 — 66,6	10^{-2}
2	50	66,6— 40	,,
3	33	40 — 28,5	,,
4	25	28.5— 22,2	,,
5	20	22,2— 18,1	,,
6	16,6	18,1— 15.4	,,
7	14,3	15,4— 13,3	,,
8	12,5	13,3— 11,7	,,
9	11,1	11,7— 10,5	,,
10			
$1 \cdot 10^{-1}$	10,0	10,5— 6,7	10^{-1}
$2 \cdot 10^{-1}$	5,0	6,7— 4,0	10^{-1}

The result E_n for the 0^{th} to 4^{th} mode is shown in fig. 28a—e. The result is as follows:

1. The maximum of energy in the longperiodic range occurs for all modes at frequencies $2 \cdot 10^{-3} - 4 \cdot 10^{-3}$ (h^{-1}) (250—500 hours).
2. The inertial waves are dominated by the first and second mode. The energy of the first mode is more than ten times larger than that of the zeroth at the inertial frequency.
3. The energy of the 0^{th} (barotropic) mode decreases with $\nu - {}^{1,4}$ with increasing frequency. Thus, the amplitude decreases with $\nu - {}^{-0,7}$ which corresponds to spectra of the tangential stress of the wind field (figs. 14—16).
4. The energy of the 1^{st} — 4^{th} mode decreases with $\nu^{-0,6}$ which yield for the amplitudes $\nu^{-0,3}$. This corresponds to spectra of the divergence and curl of the tangential wind stress (fig. 17).

From this we conclude that the driving force for all the baroclinic motions which are responsible for the great variability in the sea, are the curl and the divergence of the wind field as has been stated already theoretically (M. Tomczak, 1966, 1967; W. Krauss, 1972).

We finally reproduce in fig. 28f the ratio E_1/E_0 of the dominating 1^{st} to the barotropic 0^{th} mode. The figure demonstrates once more what has been derived already from the energy plots of fig. 25:

1. The inertial waves are dominated by baroclinic modes.
2. The barolinic first mode is larger than the barotropic mode in the period range from 10—20 hours.
3. The baroclinic effects decrease with decreasing frequency.
4. The amplitude ratio $A_1/A_0 > 0{,}5$ for periods shorter than about 40 hours.

As stated already in section 9, the period range from 10—40 hours is mainly responsible for the large variability in the Baltic Sea.

11. Current direction and velocity of the modes

The amplitudes $A_n(t)$ of the filtered records of station 1968—2, computed in section 10, have been used to compute current direction and velocity for each frequency band. The procedure is as follows:

1. $A_n^u(t)$ and $A_n^v(t)$ are computed according to section 10 for the u and v components.
2. Velocity amount and direction are obtained according to

$$\varphi_n(t) = \operatorname{arctg} \frac{A_n^u(t)}{A_n^v(t)}, \quad | \mathfrak{v}_n | = \sqrt{\left[A_n^u(t) \right]^2 + \left[A_n^v(t) \right]^2}$$

Classes of 20° width ranging from 0°—19°, 20°—39° ..... 340°—359° have been defined and the mean current velocity $|\overline{\mathfrak{v}}_n| = \frac{1}{Q} \sum_{n=1}^{Q} | \mathfrak{v}_n (t_n) |$ has been computed for each 20° sector. Thus, we obtain current "ellipses" for each mode and frequency band. These ellipses are displayed in figs. 29—31.

For periods less than 10 hours the currents are equally distributed over 360° with about equal amplitude of the 1^{st}—4^{th} mode and a slightly dominating 0^{th} mode. For periods greater than 10 hours the currents become more elliptic with a main axis from NW—SE. At the inertial frequency (13, 3—15, 4 hours) the 1^{st} and 2^{nd} mode become

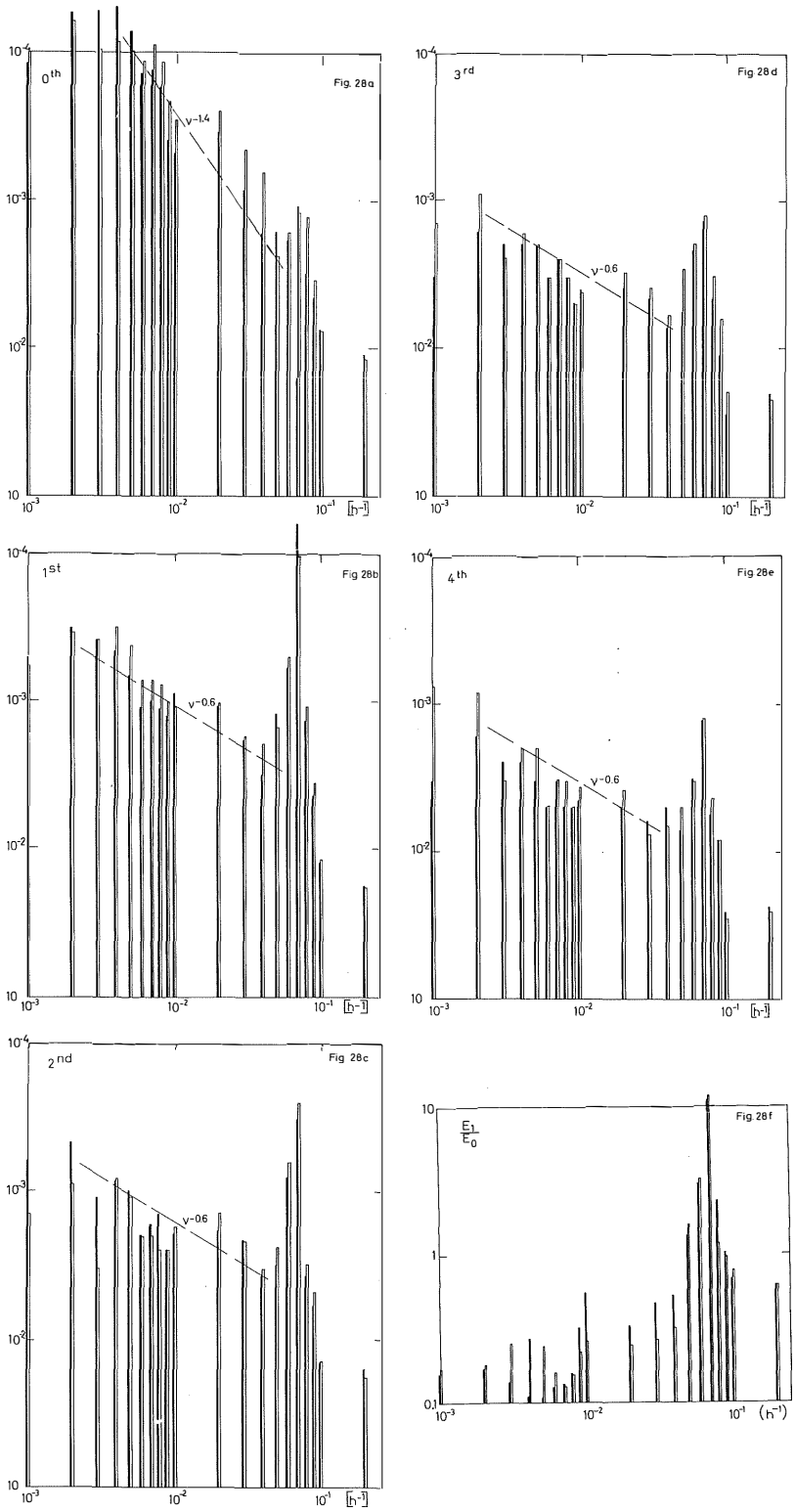

Fig. 28: Energy distribution of 0th to 4th mode at station 1968—2 (a—e) and ratio E_1/E_0 of the 1st to 0th mode (f) light line: u-component, heavy line: v-component)

Tafel 18 (zu J. Kielmann, W. Krauß u. K.-H. Keunecke)

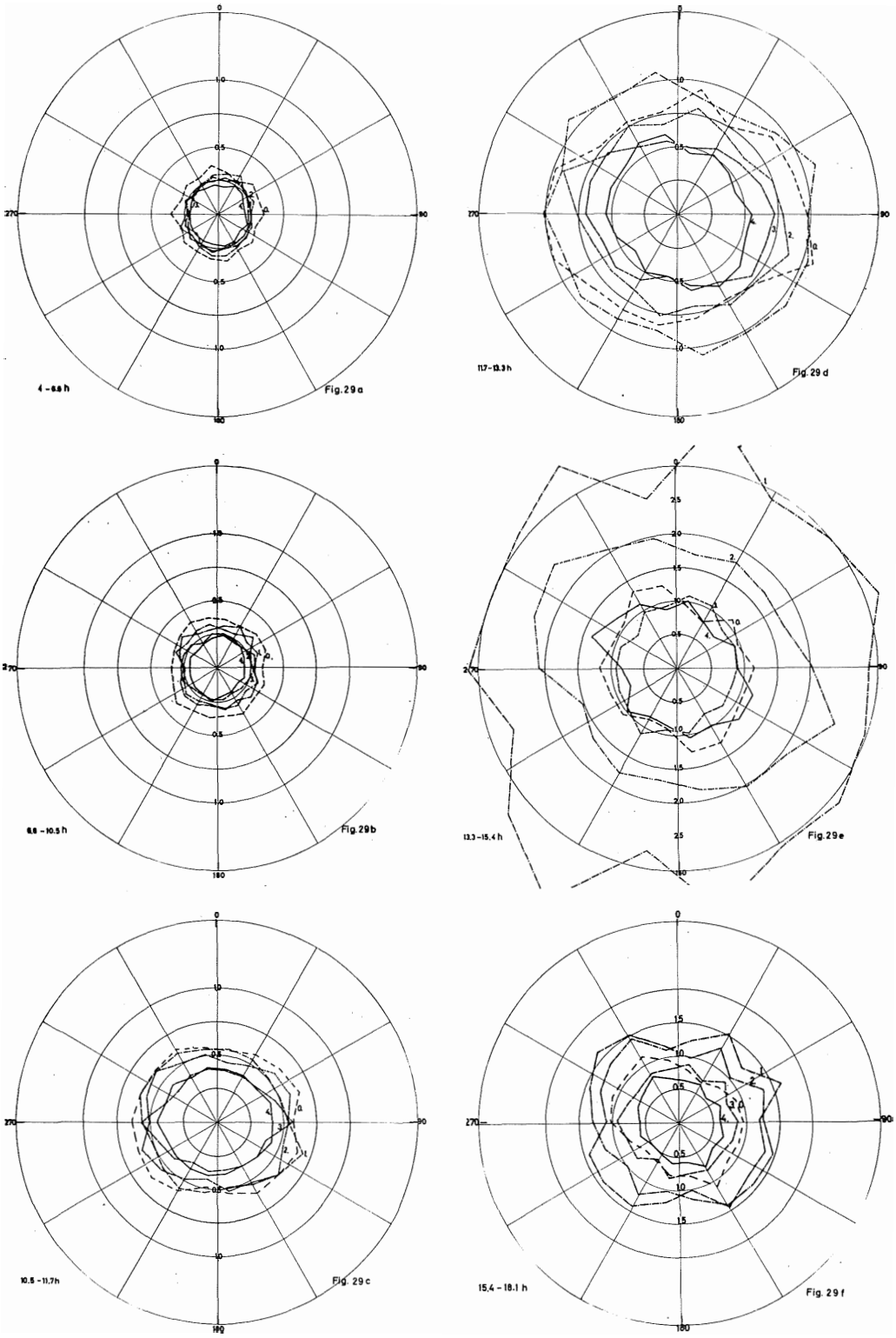

Fig. 29—31: Current ellipses for the 0th—4th mode and frequency bands given by table 4

Tafel 19 (zu J. Kielmann, W. Krauß u. K.-H. Keunecke)

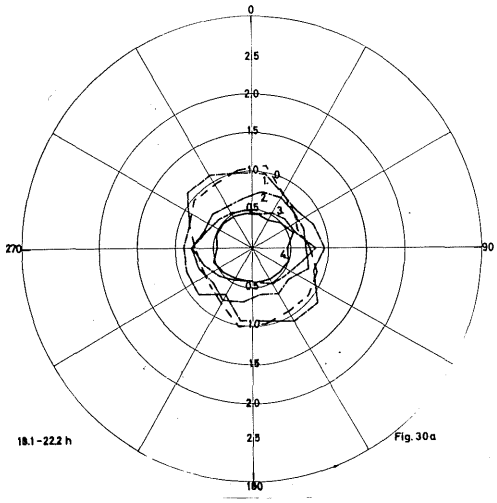

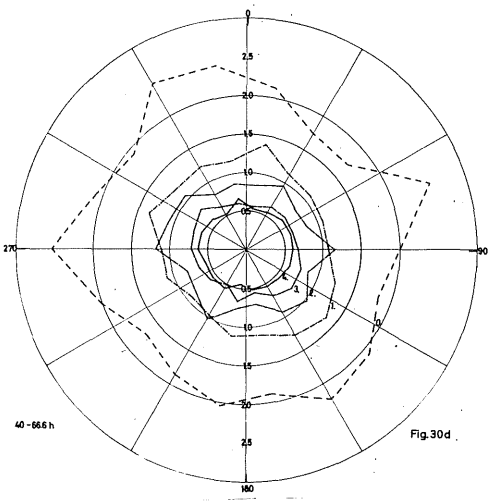

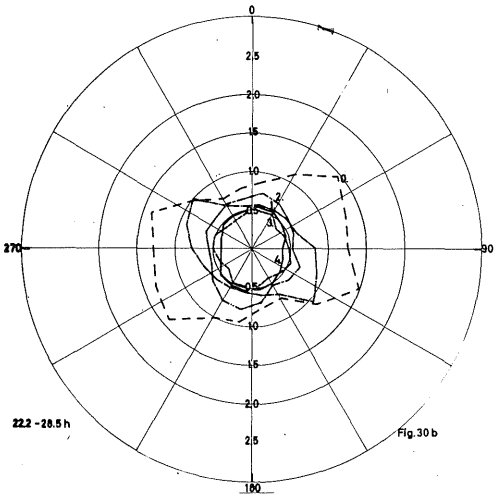

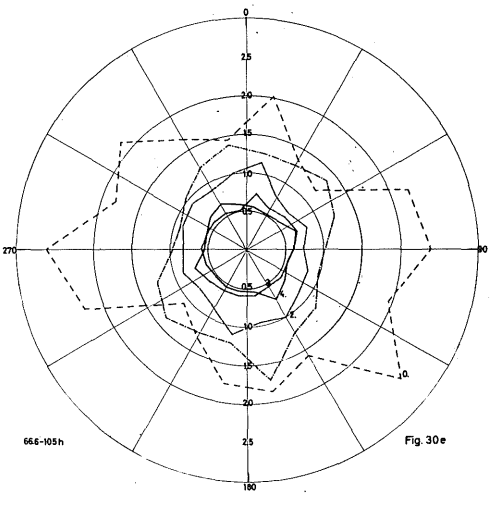

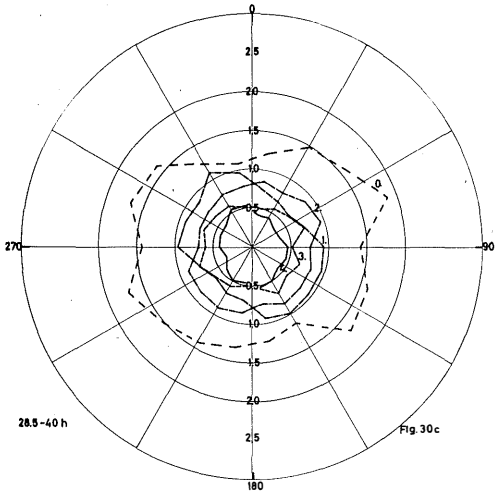

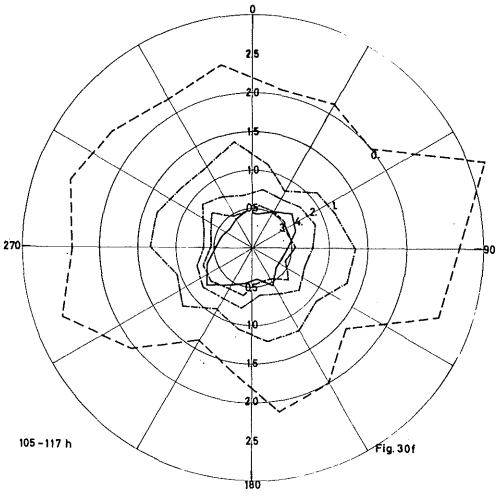

Tafel 20 (zu J. Kielmann, W. Krauß u. K.-H. Keunecke)

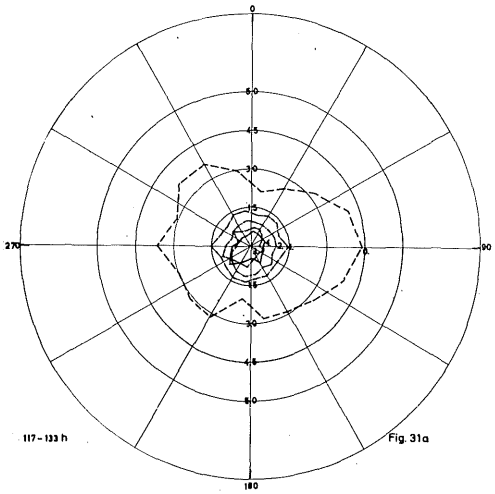

Fig. 31a

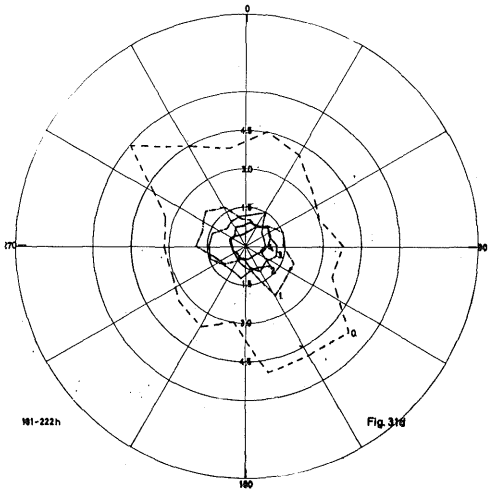

Fig. 31d

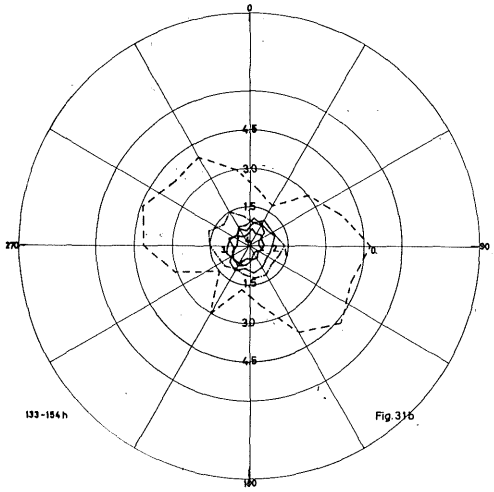

Fig. 31b

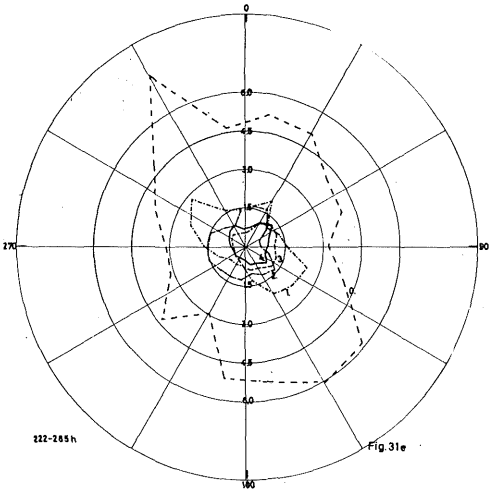

Fig. 31e

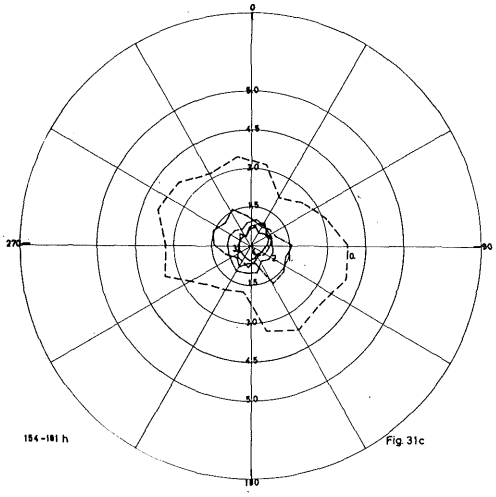

Fig. 31c

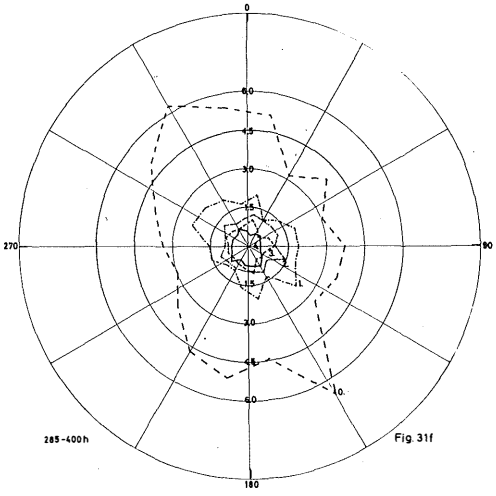

Fig. 31f

Tafel 21 (zu J. Kielmann, W. Krauß u. K.-H. Keunecke)

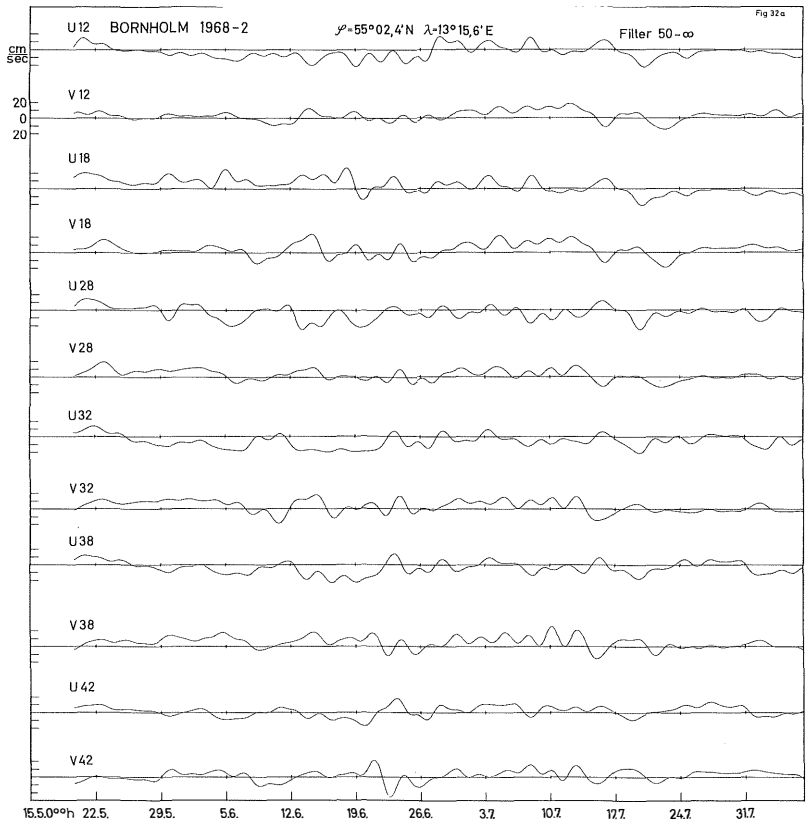

Fig. 32a, b: The long-periodic currents obtained by filtering (50 h — ∞)

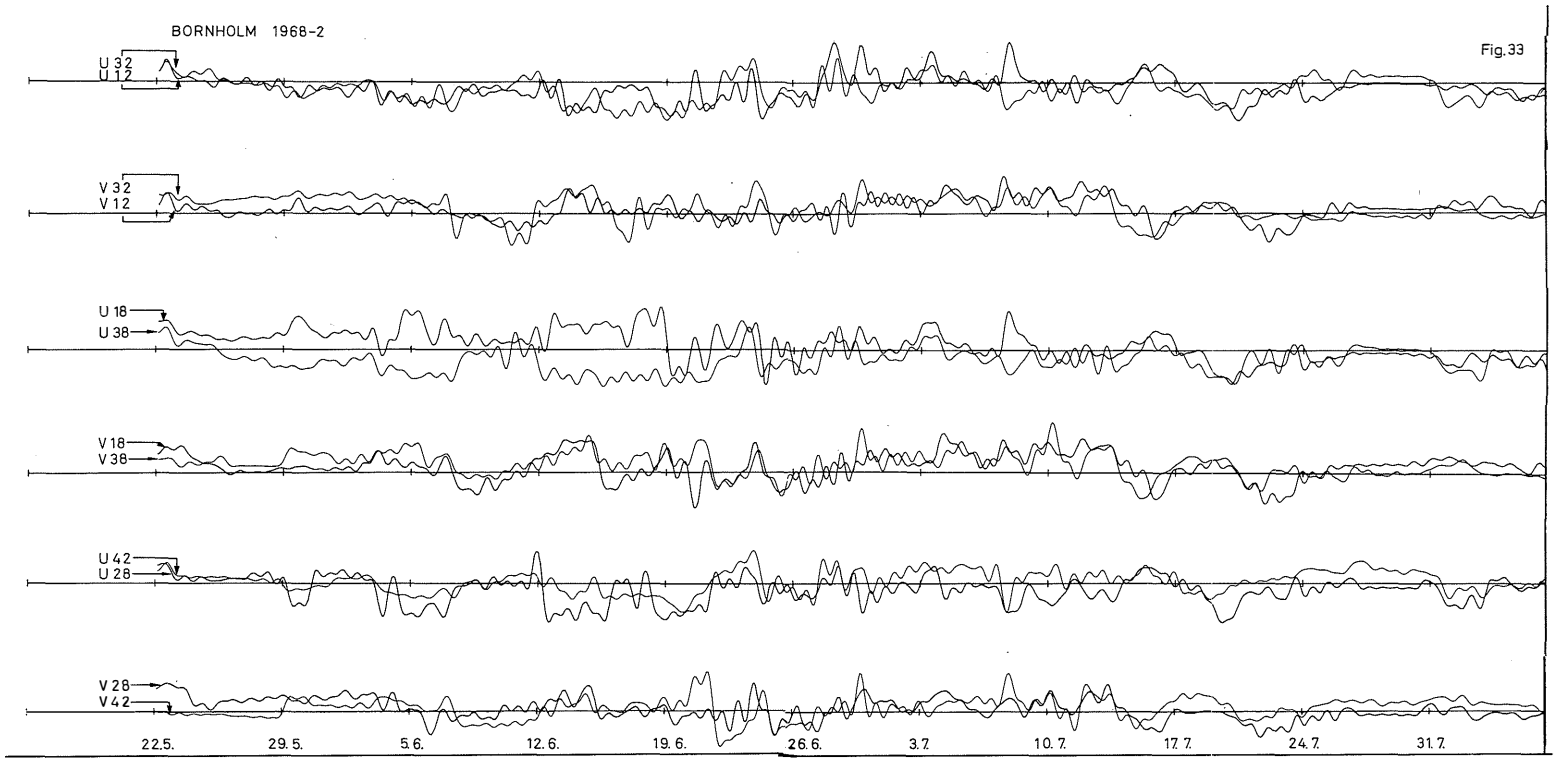

Fig. 33: Comparison of current velocities at different depths after low pass filtering 18 h—∞

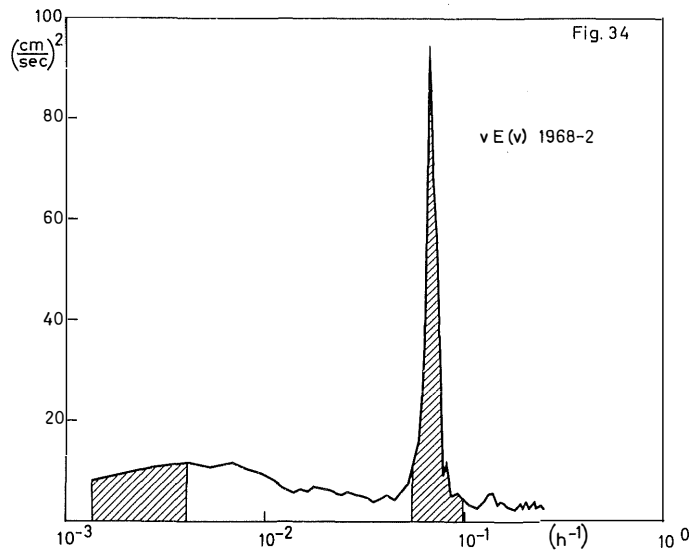

Fig. 34: Energy distribution $\upsilon E(\upsilon)$ at station 1968—2

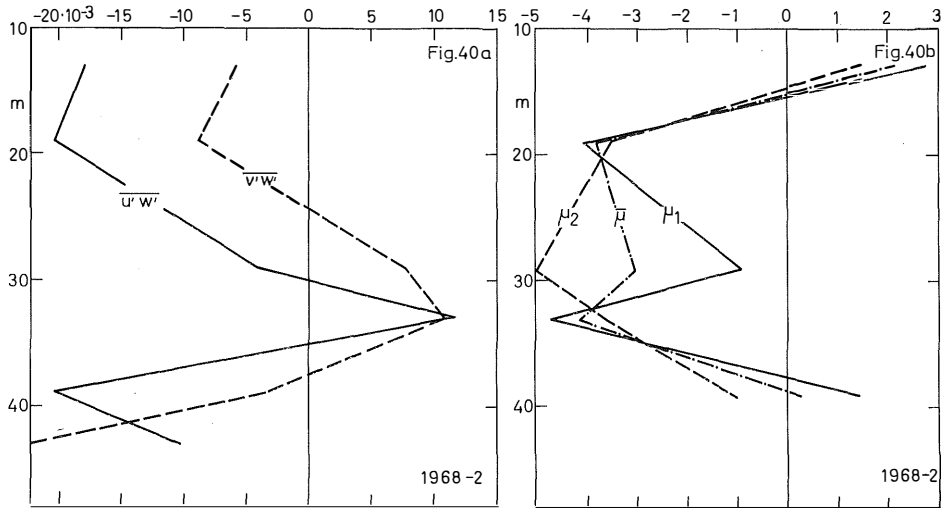

Fig. 40: Reynolds stresses u'w' and v'w' (left) and eddy coefficients μ_1, μ_2, and μ

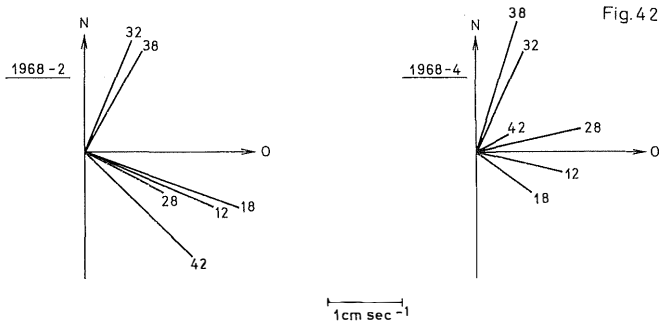

Fig. 42: Principal direction and amplitude of the seiches currents at station 1968—2 and 1968—4. (Numbers indicate depth)

Tafel 24 (zu J. Kielmann, W. Krauß u. K.-H. Keunecke)

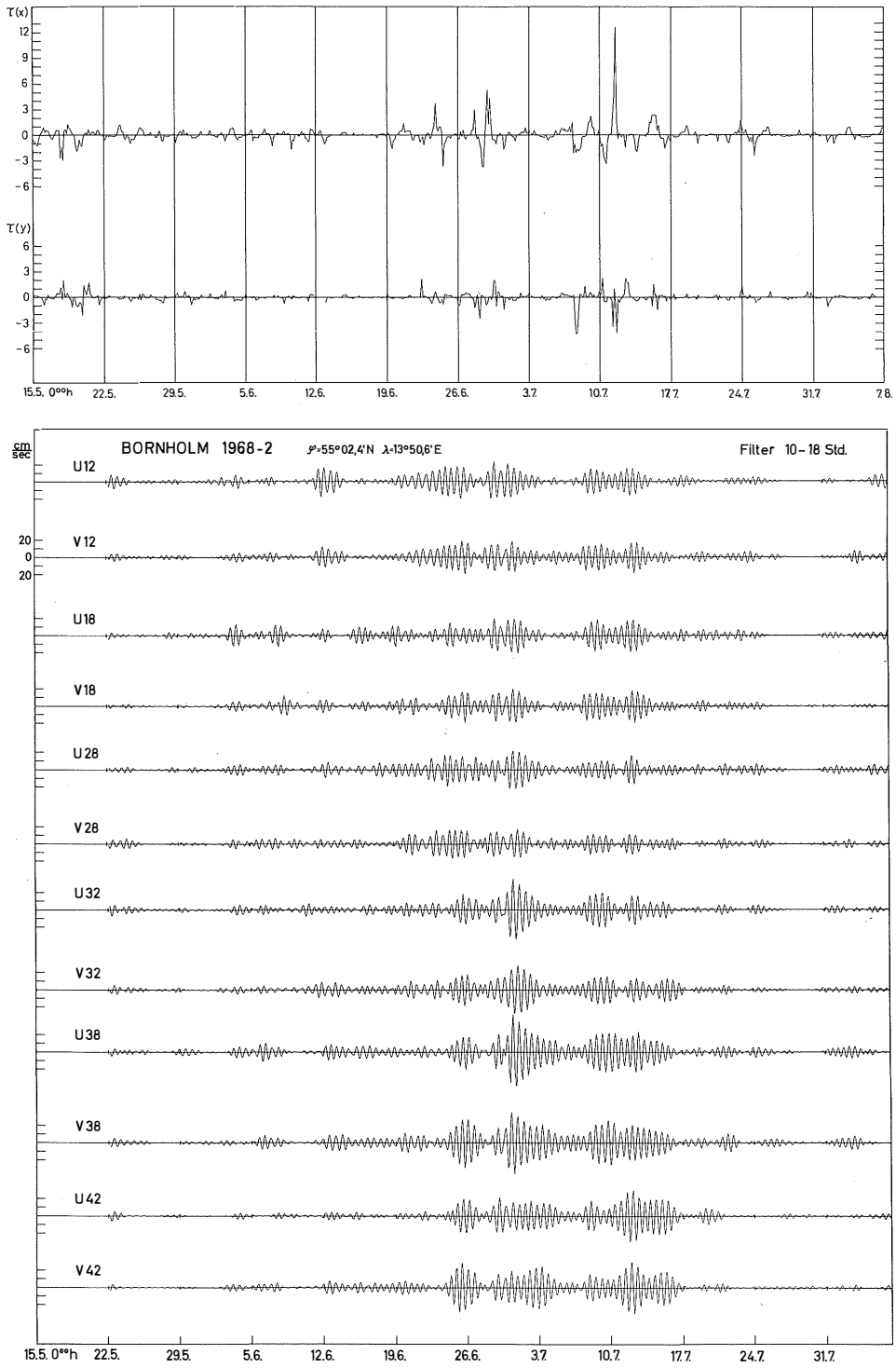

Fig. 35a, b: Filtered records (10—18 hours) of the current components at station 1968—2 (lower part) showing inertial waves and tangential stress of the wind (top)

Tafel 25 (zu J. Kielmann, W. Krauß u. K.-H. Keunecke)

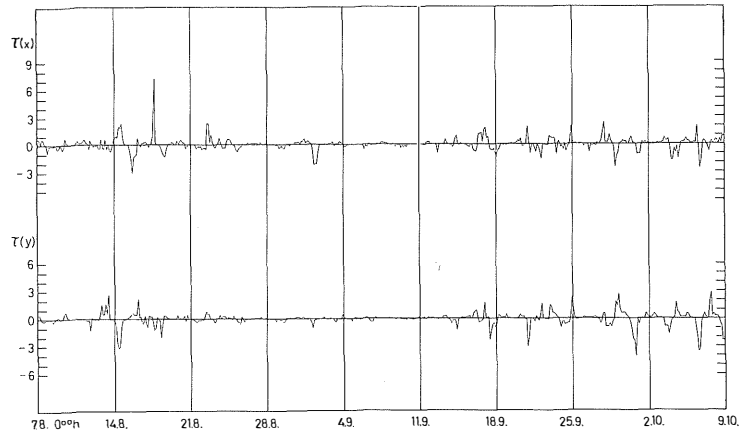

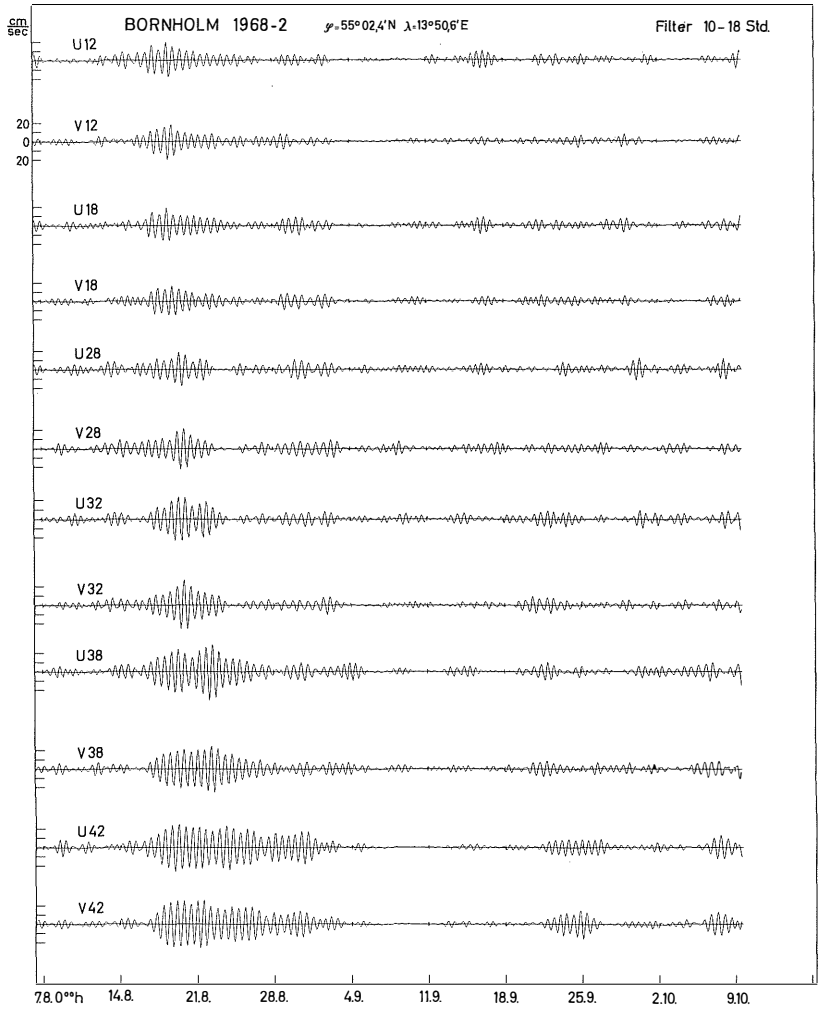

Tafel 26 (zu J. Kielmann, W. Krauß u. K.-H. Keunecke)

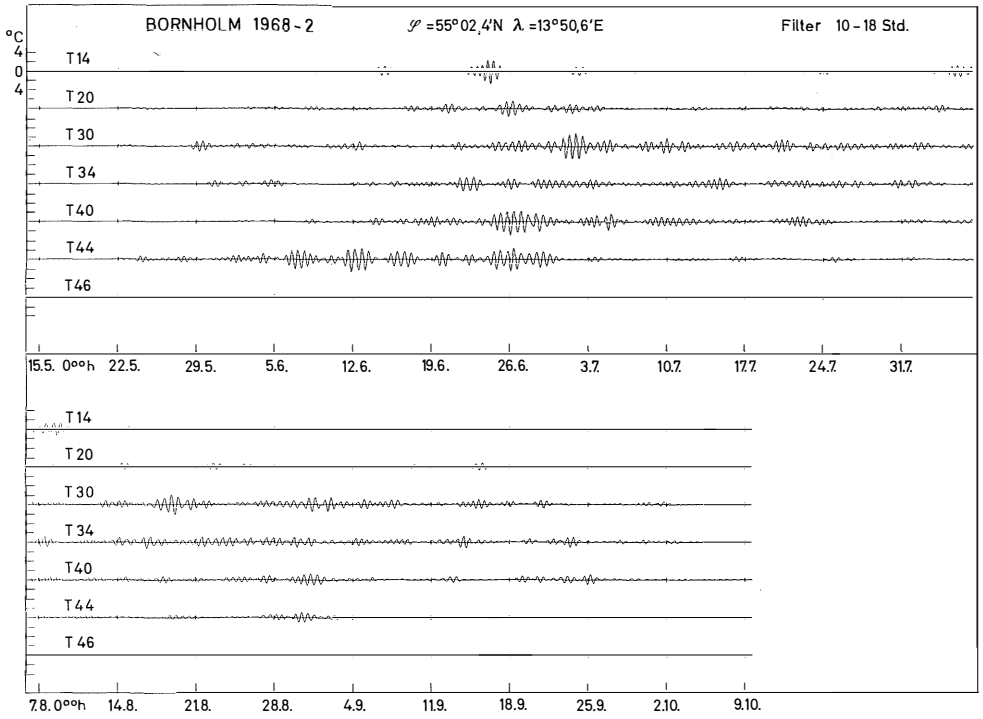

Fig. 36: Filtered temperature records (10—18 h) at station 1968—2

dominating. The main axis of the first and second mode are orientated perpendicular to one another.

In the seiches range 18 — 40 hours the 0^{th} mode increases. For 18, 1 — 22, 2 hours it is orientated perpendicular to the Rönne Bank, for longer periods the main axis of the current ellipse has the direction of the Arkona Basin. Generally, the 1^{st} and 2^{nd} mode ellipses are orientated perpendicular to one another. For periods larger than 40 hours the velocities of the 0^{th} mode increase and the internal modes decrease. The main axis of current ellipses of the 0^{th} mode turn from a W—E direction with increasing period to a N—S direction which may be interpreted in such a way that for increasing periods the currents belong more to the system Western Baltic — Gulf of Bothnia.

12. Long periodic currents

The current records of station 1968—2 have been filtered by a low-pass filter (50h — ∞) in order to study the response of the Baltic in the longperiodic range. The results are displayed in figs. 32a and b. As can be seen directly from the figures, the currents are mainly barotropic (nearly independent of depth).

According to fig. 28f this was to be expected. For longperiodic current (and sea level) prediction, the Baltic, therefore, can be treated approximately like a homogeneous water body.

The baroclinic effect becomes more important for periods less than 50 hours (fig. 28f). To demonstrate the effect fig. 33 shows filtered records for station 1968—2, low-pass filtered from 18 h — ∞, thus eliminating mainly the inertial waves. For comparision, two current components of different depth are drawn on each line. The striking differences confirm the baroclinic effects in the 18 h — 50 h period range.

13. Inertial currents

As in other areas (F. WEBSTER, 1968) the inertial currents are the dominant signal in the current records of the Baltic Sea, not only in the Arkona Basin but also in the Gotland Deep (E. HOLLAN, 1969). Fig. 34 shows the vertically averaged energy spectrum $\upsilon E(\upsilon)$ of station 1968—2. In this representation the relative areas under the spectral curve are preserved on a logarithmic scale (F. WEBSTER, 1967). The energy in the inertial frequency band corresponds to energy in the entire period range from 250—1000 hours.

In the homogeneous surface layer the inertial waves can be created directly by variable winds as obvious from the Ekman problem (V. W. EKMAN, 1923). Observations near the surface have confirmed this relationship (R. T. POLLARD & R. C. MILLARD, 1967). In the deeper layers of a stratified fluid they should be due to divergence and curl of the wind field (M. TOMCZAK jr., 1966, 1967; W. KRAUSS, 1972) which is confirmed by fig. 28.

Inertial waves are intermittent phenomena (e. g. M. TOMCZAK jr., 1969). They typically occur for 1—2 weeks. According to fig. 28f, they are the strongest baroclinic phenomena. Figs. 35a and b show at the top the tangential stress of the wind and below the filtered current records (filter 10—18 h) for station 1968—2. The exact inertial period at this station amounts to 14.6 hours.

As can be seen from fig. 35 the occurence of the beats can be closely related to time ranges of highly variable tangential stress. The beats are obviously of a baroclinic type: they are highly variable with depth.

Temperature fluctuations of inertial period are common phenomena as is evident from fig. 36 which displays the filtered temperature records at station 1968—2. They are either due to a vertical component of velocity (internal waves close to the inertial period) or due to horizontal advection by the inertial currents. The latter would include strong space inhomogeneities in the temperature field.

The baroclinity of the inertial waves has been shown by fig. 28f. We further display a mode decomposition in the time domain. The filtered velocity records (10—20 h) have been decomposed into modes at each data point. The result is shown in fig. 37 for the u-component where a different scale has been used in the upper and the lower parts of the figure. At the top the decomposition into the 0^{th}—4^{th} mode is displayed. The 1^{st} and 2^{nd} modes are dominant in all the records.

The remaining part of the figures contains (in a different scale) the original filtered time series (O), the approximation of this record by the 5 modes (A) and the difference D = O — A for each depth. As can be seen the approximation is reasonably good.

The main unknown with respect to inertial waves is their wave length. According to theory it should reflect the wave length of the curl and divergence fields of the wind which are completely unknown. Fig. 38 displays simultaneous filtered records of inertial waves at stations 1968—1, 1968—2, 1968—4 and 1968—5. There are events which occur simultaneously at several stations. But others do not.

The strong baroclinity of the waves indicates that they are mainly internal waves close to the inertial frequency. The wave length may have any value between about 10 km and several hundreds of km. Some information can be obtained from cross spectral analysis between station 1968—2 and 1968—4 which are separated by about 16,8 km. Fig. 39 displays the coherence $k = \sqrt{(C^2 + Q^2)/E_1 \cdot E_2}$ of the current components in the period range from 10—15 h (C = Cross spectrum, Q = Quadrature spectrum, E_1, E_2 energy spectra). The coherence in the seiches range between the stations is extremely poor. At the inertial frequency it increases to values of about 0.5—0.7. The mean phase lag between station 1968—2 and 1968—4 amounts to 270°, varying between 231° and 306° for all depths. Thus, the wave arrives at 1968—4 about 10.9 hours later than at 1968—2. From this we get a phase velocity of c = 42,8 cm sec^{-1} along the line which connects 1968—2 and 1968—4. The wave length obtained for the inertial waves amounts to 22.5 km which is surprisingly small but fits into the picture that the energy varies considerably even over very short distances.

14. Eddy coefficients due to inertial waves

Because of the fact that inertial currents are the strongest signal in the spectrum they should give the major contribution to the eddy coefficients efficient for long periodic fluctuations and mean currents. The eddy coefficients have been computed at station 1968—2 from the filtered records (10—18 h) of u, v, and T in the following way:

1. The filtered records are taken to be deviations u′, v′, T′ from the mean values.
2. w′ was computed according to $w' = -\frac{\partial T'/\partial t}{\partial \bar{T}/\partial z}$ where $\partial\bar{T}/\partial z$ were taken from the mean temperature profile of the mast records.
3. $\overline{u'\,w'}$, $\overline{v'\,w'}$, $\mu_1 = -\frac{\overline{u'\,w'}}{\partial\bar{u}/\partial z}$, $\mu_2 = -\frac{\overline{v'\,w'}}{\partial\bar{v}/\partial z}$

   have been computed where $\partial\bar{u}/\partial z$, $\partial\bar{v}/\partial z$ again were taken from the mean profile of the mast records.

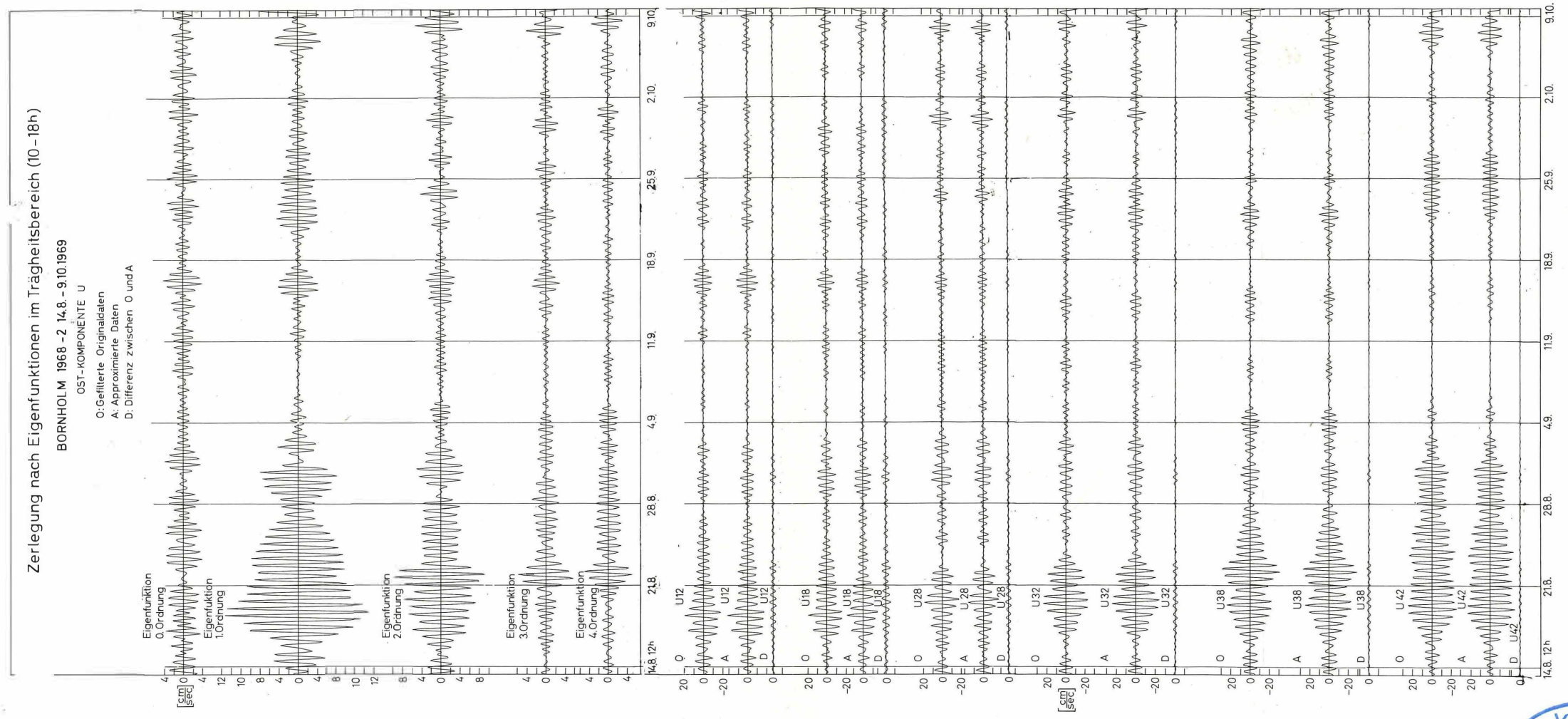

Fig. 37: Mode decomposition of the u-component at station 1968—2. Upper part: Amplitude of the 0th—4th mode in the time domain.

Lower part: Original (filtered) record (O), approximation by the modes (A) and difference D = O — A.

Tafel 28 (zu J. Kielmann, W. Krauß u. K.-H. Keunecke)

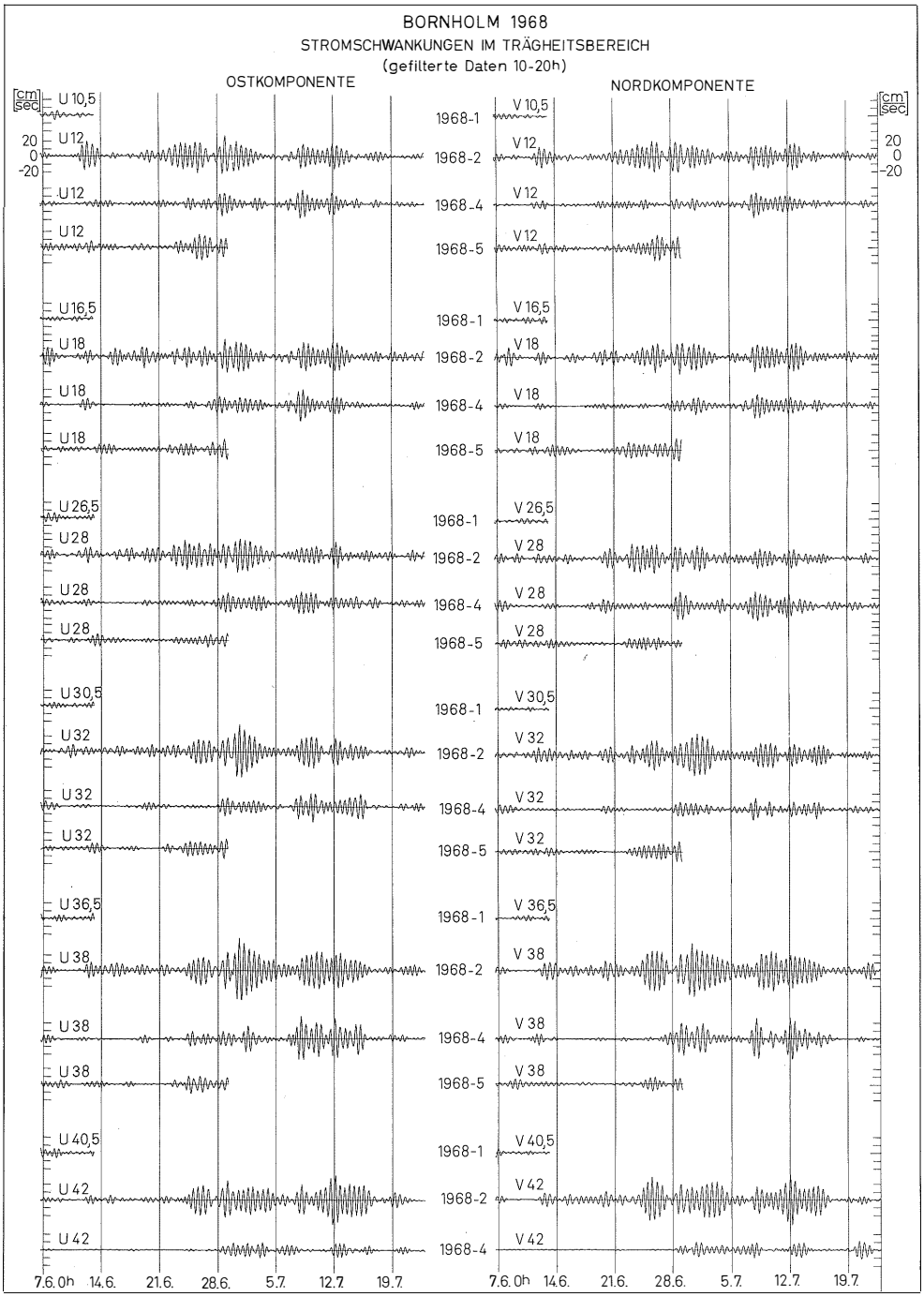

Fig. 38: Comparison of inertial waves at stations 1968—1, 1968—2, 1968—4 and 1968—5 for the time 7. 4.—19. 7. 1968

Tafel 29 (zu J. Kielmann, W. Krauß u. K.-H. Keunecke)

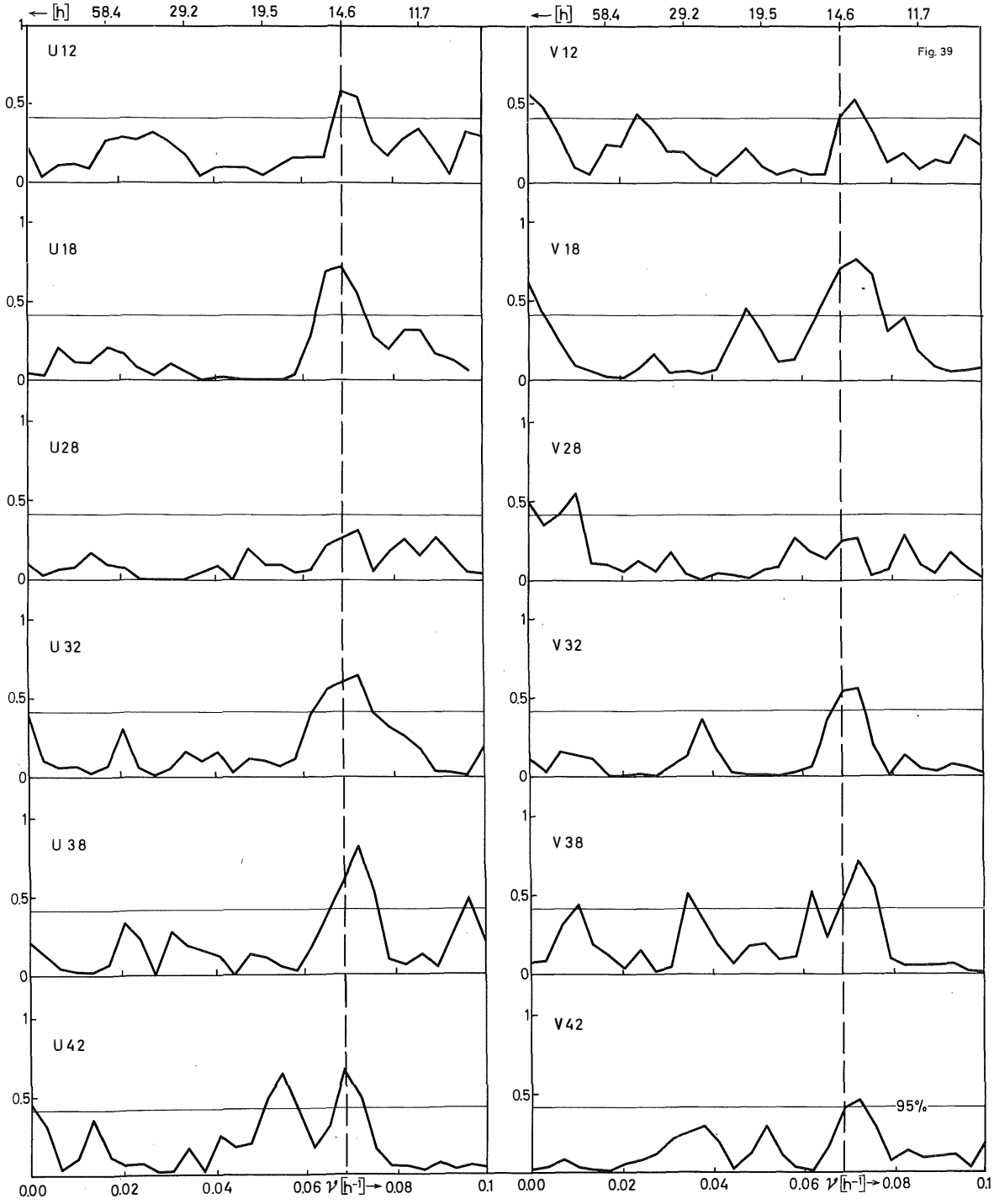

Fig. 39: Coherence between the processes at station 1968—2 and 1968—4 for periods longer than 50 hours

Tafel 30 (zu J. Kielmann, W. Krauß u. K.-H. Keunecke)

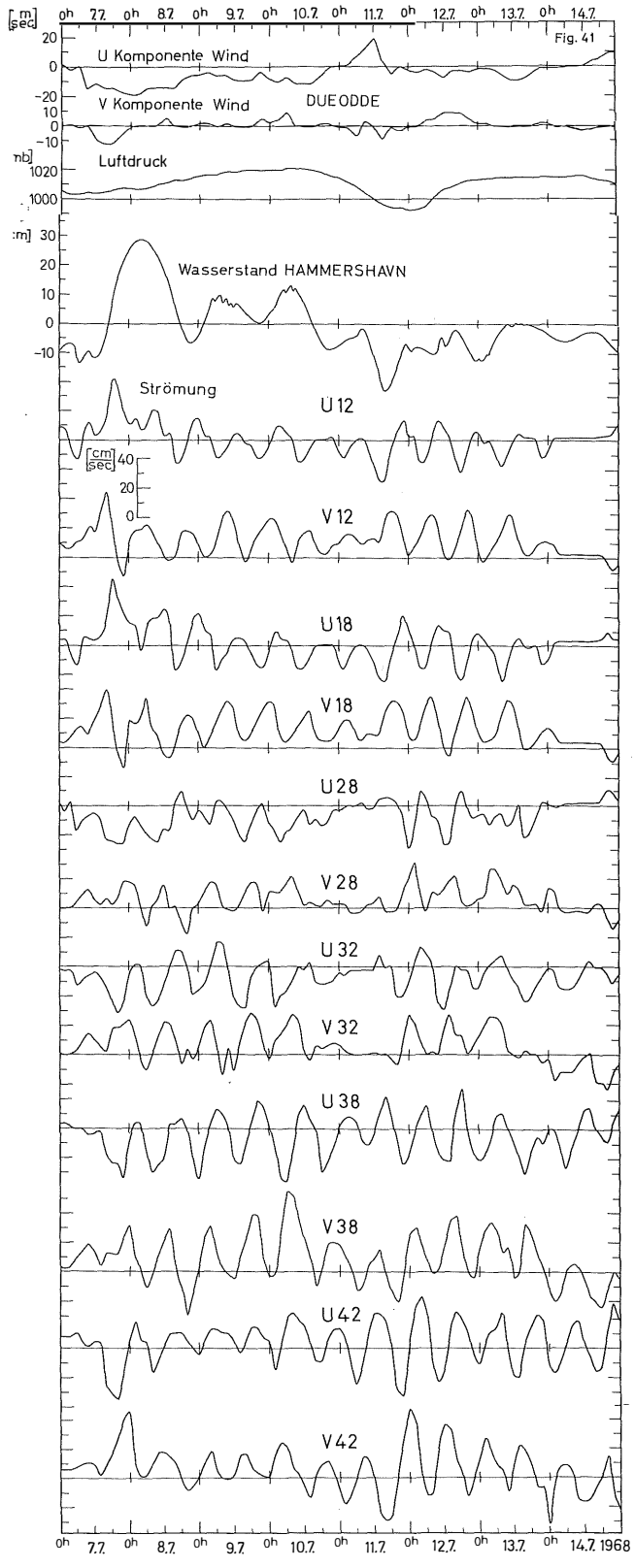

Fig. 41: Wind velocity, air pressure and sea level at Bornholm and current velocities at station 1968—2

The results are displayed in figs. 40a and b. Surprisingly, the eddy coefficient due to inertial currents is negative in the entire layer of the cold winter water which lies below the Ekman layer. Positive values are only obtained in the Ekman layer (above 15 m) and near the bottom (deeper than 38 m). $\bar{\mu}$ is the mean value of μ_1 and μ_2.

Negative viscosity means that the internal waves transfer energy to the mean currents. Thus, the motion of the cold winter water could be induced by the inertial waves.

Negative viscosity has been computed also in other areas of geophysical fluid dynamics (V. P. STARR, 1968). In the present case the result should be taken with care because the weak point in these computations is the derivation of the w′-field from the temperature fluctuations. Additionally, the recording levels for u, v and T are different as shown by table 2c. It may, howewer, be worthwhile to consider the possibility of such an energy transfer.

15. Seiches

The barotropic seiches of the Baltic Sea are wellknown (G. NEUMANN, 1941, W. KRAUSS & L. MAGAARD, 1962). They often occur, especially in connection with the 120 h fluctuations, which are due to the windfield (L. MAGAARD & W. KRAUSS, 1966). They are strongly damped, which may be due to the fact that their energy is partly lost to nonlinear seiches due to bottom friction (W. KRAUSS, 1973). Another reason may be that they loose energy to internal seiches at the sills of the Baltic.

The system of free internal seiches for a longitudinal section of the Baltic has been computed by W. KRAUSS (1963). Their wave lengths in the Arkona Basin are typically 70 and 40 km for the first and second mode, respectively. The mechanism by which they are produced is less understood. From fig. 30b (current ellipses for 22, 2—28, 5 h) we conclude, that the dominating barotropic seiche of about 27 hours is an oscillation in ENE — WSW direction and the 1st baroclinic mode is in direction SE—NW, that is nearly perpendicular to the Rönne Bank, which indicates, that the baroclinic one is induced by the bottom topography.

During summer 1968 a tide gauge was installed at Hammershavn (Bornholm island); the spectrum of the records is shown in fig. 18. The 27 h and 17 h seiches occured during the periods of 9.—16. 6. and 5.—14. 7.

The strongest seiches were observed during the time of 7. 7.—14. 7. 1968. Fig. 41 displays the meteorological conditions at Dueodde (Bornholm), the sea level variations at Hammershavn and the currents at station 1968—2.

As can be seen the currents do not reveal the seiches but are completely dominated by inertial waves. Current records, therefore seem to be not very suitable to analyse seiches in that area. The current velocities due to seiches should be about 6 cm sec^{-1} according to their amplitudes at Bornholm. This is rather small compared with the inertial currents.

Being aware of these difficulties we tried to compute the main direction of the seiches by a method independent of that used in fig. 30b.

According to Y. NAGATA (1964) the principal direction Θ of the orbital velocity of a wave field can be computed from the second moments of the velocity components,

$$\tan 2\,\Theta = \frac{2\,M_{11}\,(\omega)}{M_{20} - M_{02}} \quad ,$$

and

$$\gamma^2 = \frac{M_{20} + M_{02} - \sqrt{(M_{20} - M_{02})^2 + 4\,M_{11}^2}}{M_{20} + M_{02} + \sqrt{(M_{20} - M_{02})^2 + 4\,M_{11}^2}}$$

is a measure of the long-crestedness of the wave field. When the directions of the waves are random, $\gamma = 1$, and in case of waves with infinite long crests, $\gamma = 0$. The results for γ^2 are given in table 5 for filtered records (23—29 h) of stations 1968—2 and 1968—4.

Table 5

Long-crestedness of seiches of period 26.1 hours

depth (m)	γ^2 1968—2	1968—4
12	0.22	0.40
18	0.20	0.80
28	0.50	—
32	0.75	0.40
38	0.56	0.92
42	0.70	0.20

The principal direction and the amplitude of the seiches currents, ($\pm$ 180°) is shown in fig. 42.

At the central station 1968—2 the 26.1 h- seiche represents a long wave in the surface layer down to 18 m, which crosses the Rönne Bank. If we interpret the current ellipse of the 0th mode in fig. 30 b as a superposition of two ellipses with main axis in direction WSW — ENE and WNW — ESE, belonging to the wave field which surrounds Bornholm island north and south, then the currents in 12 m and 18 m depth would be mainly due to the 0th and 1st mode. In the deeper layer the wave arriving through Bornholm Gatt becomes dominant and the superposition of both waves (including strong baroclinic components according to fig. 30 b) yields a short-crested wave field in the Arkona Basin.

At station 1968—4, which is closer to Bornholm, we obtain in principle the same result. The wave through Bornholm Gatt becomes more dominant and, consequently, due to superposition of both main wave directions, the wave field gets more random.

Thus, it may be stated, that the seiches currents in the Arkona Basin are small compared with inertial currents and that probably Bornholm and the Rönne Bank are responsible for a very complicated structure of the wave field.

16. Temperature sections by means of towed Thermistor cables

During the survey in 1968 a preliminary type of the towed thermistor cable was used for the first time which has been described by K.-H. KEUNECKE (1972). Therefore a part of this cruise was planned to be a test for the cable and its handling aboard the R. V. "Planet". Roughly outlined, it consisted of a cable having a length of 40 m, which was equipped with 26 thermistors, equally spaced along the cable at intervals of 1,5 m. The temperatures were measured with an accuracy of $\pm$ 0,1° C and were recorded every minute on punch tape. The ship speed for the tows varied between 4 and 7 kn. The angle between the horizontal coordinate and the cable was 45°—60° depending on the speed. Hence temperature profiles were recorded only in the upper layer extending from the surface to depths of 30—33 m.

It turned out that the instrumentation worked fairly well. Therefore the observed spatial distribution of the temperatures could be a useful supplement to the previously described measurements in the Arkona Basin. However it is wellknown from many authors (e.g. W. KRAUSS, 1966c; K. D. SABININ, 1969) that the interpretation of data from a towed instrument is a crucial problem. In general, such observations do represent

Tafel 31 (zu J. Kielmann, W. Krauß u. K.-H. Keunecke)

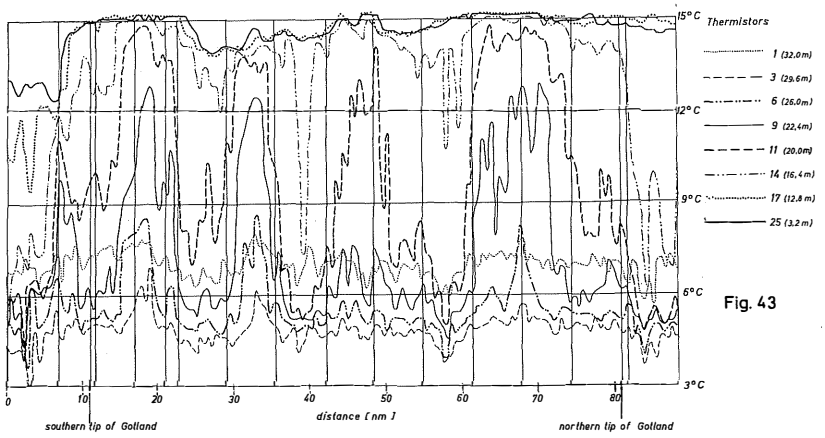

Fig. 43: Temperature records during towing course 2 at the depths 3.2 m, 16.4 m, 20.0 m, 22.4 m, 26.0 m, 29.6 m, 32.0 m

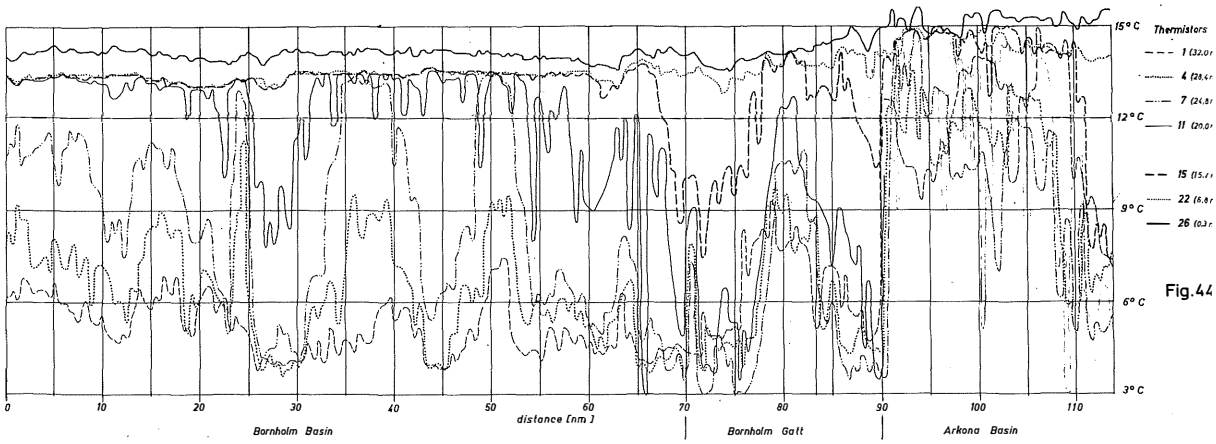

Fig. 44: Temperature records during towing course 3 from Bornholm Basin to Arkona Basin at the depths 3.2 m, 16.4 m, 20.0 m, 22.4 m, 26.0 m, 29.6 m, 32.0 m

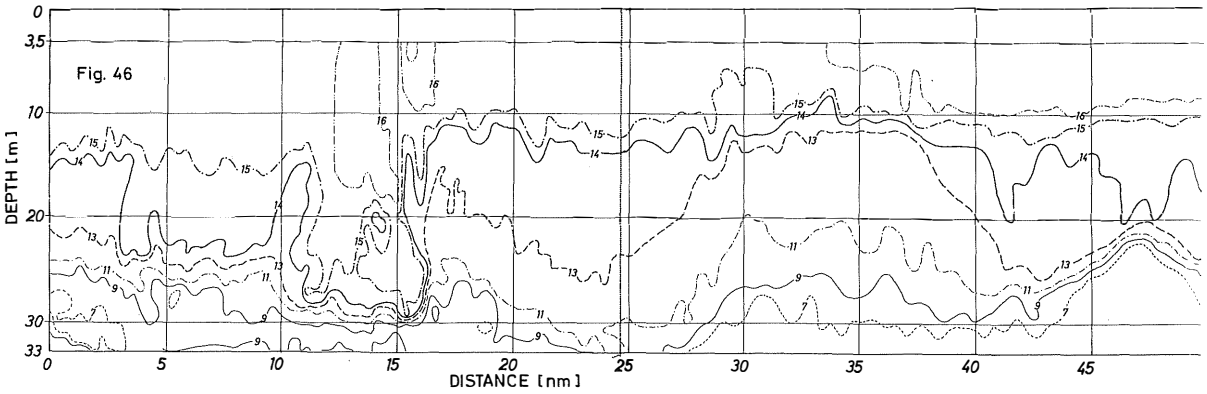

Fig. 46: Temperature stratification in the Arkona Basin, July 10—11.

Tafel 32 (zu J. Kielmann, W. Krauß u. K.-H. Keunecke)

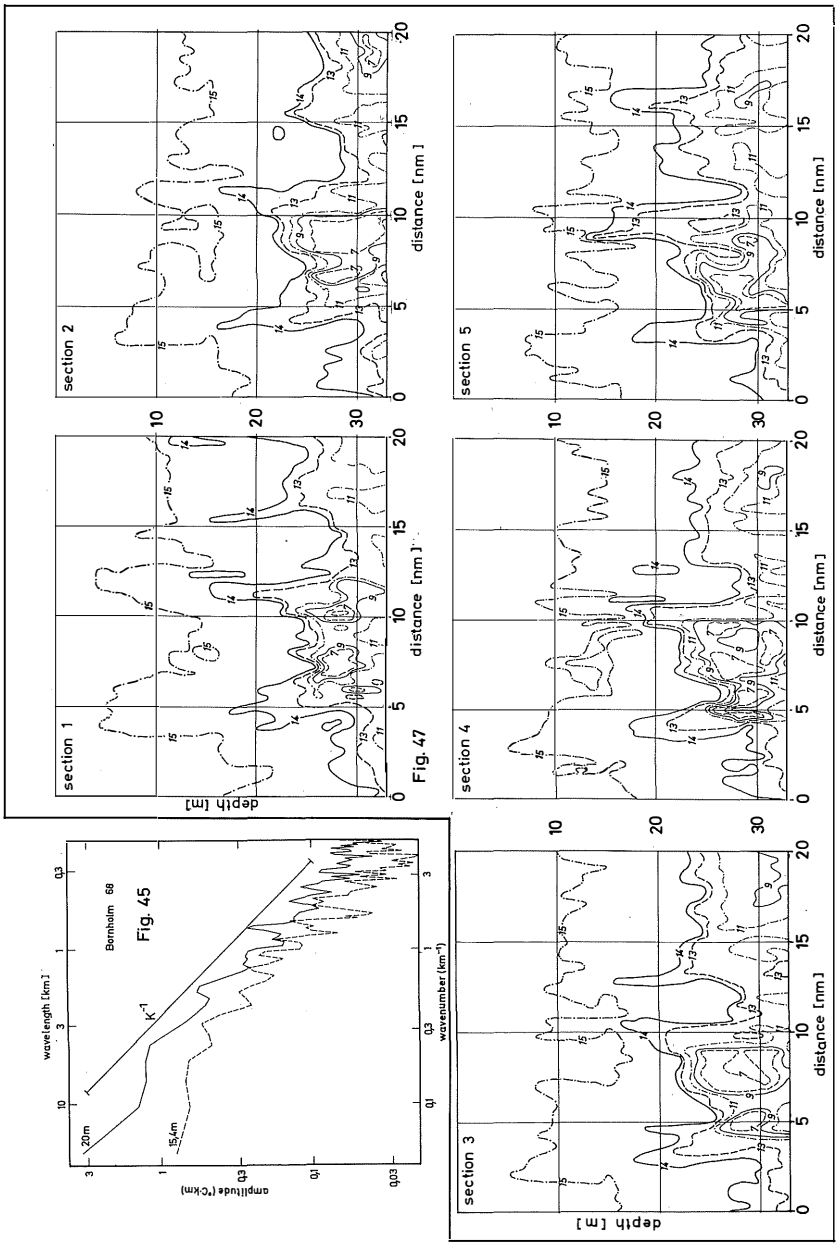

Fig. 45: Amplitude spectra of the temperature fluctuations during course 3 at 15.4 m and 20 m

Fig. 47: Repeated measurements of the temperature stratification in the Arkona Basin, July 21—22

neither the true spatial distribution at a definite time nor the actual temporal fluctuations, but a superposition of both. Furthermore the temperature stratification in the Baltic Sea is much more complicated than in the ocean, because of the very different water masses and the bottom topography.

During July 1968 the thermistor cable was used three times. The courses are shown in fig. 3. At first on July 3—5 (course 1) two temperature sections had been made in the Arkona Basin. The measurements were continued from July 10—11 in the Midbaltic (course 2). The cable was towed from the southern tip of Öland (56°10′ N, 16°35′ E) west of the island Gotland to the latitude of Stockholm (59°20′ N, 17°10′ E). Course 3 was made from the position 58°35′ N, 20°40′ E through the Midbaltic to the Arkona Basin (55°03′ N, 13°50′ E) on July 15—17. Finally five temperature sections were made along course 4, July 21—22.

The long sections (course 2 and 3) show the expected and wellknown summerly temperature stratification of the Midbaltic Sea. Below a thin mixed surface layer of a depth of about 15 m a strong thermocline extends from 15 m to 25 m. The vertical temperature gradient amounts up to 1—2 °C/m. Below the thermocline the gradient decreases to about 0,1°C/m. The temperature difference between the uppermost thermistor at the surface and the deepest one at 32 m varies between 12°C and 15°C. In these temperature sections considerable horizontal temperature gradients occur as can be seen from the two examples in fig. 43 and fig. 44. They show the temperatures of 8 thermistors at depths of 3.2 m, 12.8 m, 16.4 m, 20.0 m, 22.4 m, 26.0 m, 29.6 m, 32.0 m.

Fig. 43 shows the records west of the island Gotland during course 2 along a distance of 76 nm. The temperature fluctuations have a typical wave length from less than 1 nm up to 20 nm. The short fluctuations seem to have no distinguished wavelengths. This example has been chosen because of the obviously periodical deformation of the thermocline. In this record the temperature variations of about 7°C at a depth of about 20 m correspond to vertical displacements of the thermocline of approximately 15 m. The shown features are probably produced by an internal wave. Assuming that the speed of the ship of 7 kn is large compared to the phase velocity of the wave, a wavelength of 16 nm can be read off the observation. However there is no information on the frequency of the wave. But it is likely that an internal wave of this wavelength is an internal seiche. The wavelike pattern was observed along course 2 only in that part of the section which is shown in fig. 43.

In order to consider the spectral wavenumber distribution of the temperature fluctuations amplitude spectra have been calculated from two temperature series of course 2 (363 nm). The position of the first thermistor was 15,4 m just below the mixed surface layer while the second, at 20 m depth, was situated approximately in the center of the thermocline. The amplitude spectra (fig. 45) of these series do not show any significant peak at a specific wavelength.

For wavelengths of less than 3 km the amplitudes decay approximately proportional to K^{-1}, when K is the wavenumber. The obvious oscillations as shown for example in fig. 43 occur only with a few wave trains and their spectral contribution therefore is negligibly small.

During July 1968 the described temperature stratification of the Midbaltic Sea was quite different from that of the Arkona Basin. This can be seen from fig. 44, where the course 2 temperatures are shown (from Bornholm Deep to Arkona Deep). At the left hand side there is still the typical temperature distribution which has been observed along course 2 and 3 in the Midbaltic. Already in the Bornholm Gatt the thermocline becomes more diffuse. It extends from 15 m to 30 m, and its strength decreases. Additionally, inversions occur below the thermocline. The water of the Arkona Basin has a totally

different temperature stratification, as can be seen at the right hand side of fig. 44. Here, the strong thermocline has disappeared. Below a depth of 25 m strong inversions of about 3°C, occasionally of 5°C, occur. The direct presentation of the temperature fluctuations at selected levels does not give satisfactory information in case of such a complicated temperature structure as has been found in the Arkona Basin. However, one important feature is seen from fig. 44: The transition between the different types of water happens rapidly over a very short distance. Especially, the transition zone between the water of the Bornholm Gatt and the Arkona Basin is clearly marked by a thermal front. The extension of this transition zone is less than 1 nm. The inclination of the front is approximately 1°—2°.

The most detailed investigations with the thermistor cable have been carried out in the Arkona Basin. The temperature sections of course 1 are presented in fig. 46. Here, the isotherms are plotted instead of the temperature at a constant depth. They have been calculated by linear interpolations from the temperatures of the 26 thermistors. This section as well as those of fig. 47 reveal a very complicated temperature stratification. The depth of the thermocline varies between 12 m and 28 m. In some cases a thermocline does not even exist. The temperature gradient is rather constant, from below the mixed surface layer down to the lowest thermistor.

In the western part of the section in fig. 46 there is an intrusion of warm and obviously saline water, over a distance of 4 nm. The 11° and 13° isotherms show a wavelike pattern which is disturbed only by the intrusion. The corresponding periodic vertical displacement of about 15 m of these layers in a mean depth of 20—30 m has probably been produced by a long internal wave. The wave length is approximately 20 nm which is nearly one third of the length of the Arkona Deep. It is likely that this wave is an internal seiche.

This situation in the Arkona Basin changed considerably on July 21—22, as can be seen from fig. 47. The mixed layer has incraesed in thickness to nearly 25 m. Furthermore, temperature inversions of more than 3°C occured. These inversions were not found all over the area of investigation, but they were confined to certain locations. In order to observe the temporal variability of this temperature structure 5 repetitions of course 4 have been carried out (fig. 47). It turned out that the characteristic pattern of the isotherms appeared every time at the same position in the sections. Hence, this thermal structure has been surprisingly stationary during the time of observation of 25 hours. The pattern was probably produced by warm saline water from the North Sea. This inflow must have happened shortly before the observation, because the saline water is still clearly separated from the ambient water of the Arkona Basin by strong temperature gradients.

These few examples of spatial temperature distribution in the Baltic Sea may demonstrate that the often used assumption the mean stratification to be only a function of depth is a very rough approximation. Numerous processes may be responsible for this considerable variability.

The amplitude spectra of fig. 45 do not show distinct energy peaks. However, the original records reveal wave patterns for small wavenumbers which may be internal seiches. They appear only with a few wave trains and are, thus, restricted to small regions in the sea.

Several observed phenomena seem to be stationary at least during a few days. In some cases they represent boundaries between two types of water. Such boundaries can even have the form of thermal fronts, as has been demonstrated. The transition zone is in general small and marked by strong temperature gradients. These gradients do not change during a period of 25 hours. Therefore, it can be supposed that mixing

processes are very weak below the Ekman layer which would be expected from the results in section 14.

In regions of strong quasi-stationary horizontal temperature gradients probably also horizontal density gradients occur which must be balanced by geostrophical motions.

It is evident that the time scale of the major spatial structure must be larger than that of the internal waves. Based on this fact a method has been developed (K.-H. KEUNECKE, 1973), which allows under certain conditions the seperation of the spatial quasi-stationary structure from the temporal fluctuations, especially internal waves, by repeated sections.

17. Conclusions

From the observations we have carried out during 1962—1968 (mainly in the Arkona Basin) we have learnt, that for periods larger than about 20 hours the barotropic response is dominating, but amounts to approximately 50% even for periods of 100 hours only. Thus, models of a homogeneous Baltic Sea would give only a crude information on the currents and the corresponding hydrographic fluctuations present.

The main baroclinic range is 10—40 hours. The phenomena in that range are little understood. The main reason is that no information is available on the divergence and curl field of the tangential stress of the wind field. A meteorological buoy system for scientific purposes is urgently needed. Divergence and curl obviously reach maximum values during the passage of meteorological fronts. These, however, have not been studied yet on the ocean. As long as these informations are not available, there is little hope to interpret this major baroclinic range, which includes the inertial waves, the dominant signal in the Baltic Sea.

The main results of our research during 1962—1968 may be taken from the summary. A great deal of effort was wasted due to interference with commercial fishery. The informations we hoped to obtain in 1968 from the correlation distances are completely missing, and there is little hope, that future programs along that line would be more successful.

The main effort for future studies should lie on the observation of single events. The general shape of spectra as function of frequency is known. From fixed stations there is little hope to obtain the wave number spectrum. The same holds for towed thermistor chains in that respect, because ships are too slow to measure the range between 10—40 hours. They are suitable, however, to get the quasi-stationary patterns if powerful methods are found to surpress the entire spectrum of short-periodic (< 40 h) fluctuations.

The towed thermistor records show that large inhomogeneities remain stationary over quite long periods. The reason is not understood.

Bornholm island and the Rönne Bank seem to have a great influence on the conditions in the Arkona Basin. The influence of bottom topography on the processes should be studied in more detail. Under the study of single events we therefore mainly understand:

1. The response of the sea to the passage of meteorological fronts
2. The influence of bottom topography on the processes which occur
3. The maintenance of quasi-stationary fronts.

Appendix

The decomposition of wind-generated current fields into modes is possible in the entire frequency range 1) as long as the local Brunt-Väisälä frequency is much larger than the frequency of the fluctuations, $N >> \omega$, and 2) if the current measurements are taken below the Ekman layer in layers, where viscosity can be ignored.

The Baltic Sea can be considered as consisting of a homogeneous Ekman layer ($0 < z < h$) of about 10—15 m thickness and a stratified layer beneath ($h < z < H$). According to W. KRAUSS (1972), wind fields variable in time and space create an Ekman suction at the top h of this stratified layer given by the convolution integral between an inertial frequency wave e^{ift} and the curl and divergence of wind stress $\vec{\tau}$,

$$(1) \qquad W_h(x, y, t) = \frac{1}{\rho_I} \int_0^t \left\{ \operatorname{div} \vec{\tau}(x, y, t - \zeta) \cos f\zeta + \vec{\tau}(x, y, t - \zeta) \sin f\zeta \right\} d\zeta$$

This Ekman suction drives the lower layer. For this we have the equations (W. KRAUSS, 1966, p. 137ff)

$$(2) \quad \begin{cases} u_z + fv + \frac{1}{\tilde{\rho}} p_x = 0 \\ v_t - fu + \frac{1}{\tilde{\rho}} p_y = 0 \\ -g\rho + p_z = 0 \\ \rho_t + \tilde{\rho}_z w = 0 \\ u_x + v_y + w_z = 0 \end{cases}$$

from which

$$(3) \left(\frac{\partial^2}{\partial t^2} + f^2 \right) \frac{\partial^2 w}{\partial z^2} + g\Gamma \triangle_h w = 0$$

follows if $\Gamma \frac{\partial w}{\partial z}$ is neglected (just for simplicity). By means of Fourier transformation

$$(4) \quad f(x, y, z, t) = \int_{-\infty}^{+\infty} \int_{-\infty}^{+\infty} F(\varkappa, \eta, z, t)\, e^{i(\varkappa x + \eta y)}\, d\varkappa\, d\eta$$

we obtain for $h < z < H$ (H = bottom)

$$(5) \quad W_{zz\,tt} + f^2 W_{zz} - N^2(z) k^2 W = 0$$

where $k^2 = \varkappa^2 + \eta^2$ and $N^2 = (g/\tilde{\rho})\, d\tilde{\rho}/dz$
is the Brunt-Väisälä frequency.

The boundary conditions for (5) are

$$(6) \qquad W(k, z = h, t) = W_h(k, t),\ W(k, z = H, t) = 0$$

By means of

$$(7) \qquad W(k, z, t) = \frac{H - z}{H - h} W_h(k, t) + \tilde{W}(k, z, t)$$

we then obtain

$$(8) \quad \tilde{W}_{zz\,tt} + f^2 \tilde{W}_{zz} - N^2 k^2 \tilde{W} = N^2 k^2 \frac{H - z}{H - h} W_h(k, t)$$

and

$$(9) \qquad \tilde{W}\,(k, t) = 0 \quad \text{for } z = h \quad \text{and} \quad z = H.$$

Thus, the velocity field in the lower layer is a forced velocity field, the distribution of which depends on the vertical structure of the driving term in (8).

Formally, we can get a solution of (8) by decomposition into modes φ_n of the entire water column, which have amplitudes $\varphi_n(h)$ at the level h,

$$(10) \qquad \tilde{W}\,(k, z, t) = \sum_n A_n\,(k, t)\,\varphi_n(z), \quad \frac{H - z}{H - h} = \sum B_n\,\varphi_n\,(z)$$

where $\varphi_n\,(z)$ is given by

$$(11) \qquad \varphi_n''\,(z) + N^2\,\upsilon\,\varphi\,(z) = 0, \; \varphi = 0 \quad \text{for } z = 0 \quad \text{and} \quad z = H.$$

The amplitudes $A_n(t)$ result from

$$(12) \qquad A_n''\,(k, t) + \left(f^2 + \frac{k^2}{\nu}\right) A_n\,(k, t) = -\frac{k^2}{\nu}\,B_n\,W_h\,(k, t)$$

and read

$$(13) \qquad A_n\,(t) = -\int_0^t \frac{k^2}{\sqrt{\nu\,(f^2\,\nu + k^2)}}\,B_n\,W_h(k, \zeta)\,\sin\sqrt{\frac{f^2\,\upsilon + k^2}{\nu}}\,(t - \zeta)\,d\zeta$$

The entire solution is

$$(14) \qquad w\,(x, y, z, t) = \int_{-\infty}^{+\infty}\int \left[\frac{H - z}{H - h} W_h\,(\varkappa, \eta, t) + \sum_n A_n\,(\varkappa, \eta, t)\,\varphi_n\,(z)\right] e^{i(\varkappa x + \eta y)}\,d\varkappa\,d\eta$$

which consists of a barotropic mode (1st term) and the internal modes (2nd term).

Thus, the forced velocity field in the stratified layer beneath the Ekman layer is considered to be built up in the following way:

1. Divergence and curl of the wind stress create an Ekman suction at the top of the lower layer, which is decomposed into Fourier components with respect to x, y. The amplitude of each Fourier component is determined by the wind field.
2. Each Fourier component of the Ekman suction yields a forced velocity field with the same wavelength but a complicated vertical structure in the lower layer. This structure is formally described by the modes of the entire water column.

In section 10 this mode decomposition is carried through at a distinct position x_0, y_0, but with respect to the horizontal velocity components, which are decomposed into the modes $d\varphi_n/dz$.

There is a striking difference between common mode theory used in the theory of internal waves and the way it is used in this context:

Free internal modes depend only on the stratification. But a definite relation exists between the frequency and the wave number of each mode, which limits the existence of the modes to the frequency range $f < \omega < N$!

In the present context the forced velocity field is formally decomposed into the same modes, depending only on the stratification. But there is no definite wavelength which corresponds to each mode. On the contrary, for each wavelength of the forced velocity field a mode decomposition is possible.

The modes could not exist as individual sin waves. What exists in reality is a forced field which depends on the meteorological conditions. The easiest way to describe this field is to describe it by a number of modes (as common in other fields of physics).

Literature

DEFANT, A. (1960): Physical Oceanography Vol. 2. Pergamon Press, Oxford, 598 pp.

EKMAN, V. W. (1923): Über Horizontalzirkulation bei winderzeugten Meeresströmungen. Arkiv för Matematik, Astr. och Fysik **17**, 26; 74 pp.

HELA, I. & W. KRAUSS (1959): Zum Problem der starken Veränderlichkeit der Schichtungsverhältnisse im Arkona-Becken. Kieler Meeresf. XV, 125—143.

HOLLAN, E. (1969): Die Veränderlichkeit der Strömungsverteilung im Gotland Becken am Beispiel von Strömungsmessungen im Gotlandtief. Kieler Meeresf. XXV, 1, 19—70.

JACOBSEN, J. P. (1925): Die Wasserumsetzung durch den Öresund, den Großen Belt und den Kleinen Belt. Medd. f. Komm. f. Havunders. Ser. Hydr. Bd. II, 9, Kopenhagen.

KÄNDLER, R. (1951): Der Einfluß der Wetterlage auf die Salzgehaltsschichtung im Übergangsgebiet zwischen Nord- und Ostsee. Dtsch.Hydrogr. Z. **4**, 150—160.

KEUNECKE, K.-H. (1972): Ein Schleppkabel zur Messung räumlicher Temperaturprofile. Kieler Meeresf. XXVIII, 39—44.

KEUNECKE, K.-H. (1973): On the observation of internal tides at the continental slope off the coast of Norway. "Meteor" Forsch. Ergebnisse: A, 12, 24—36.

KIELMANN, J. W. KRAUSS und L. MAGAARD (1969): Über die Verteilung der kinetischen Energie im Bereich der Trägheits- und Seichesfrequenzen der Ostsee im August 1964 (Internationales Ostseeprogramm). Kieler Meeresf. XXV, 245—254.

KRAUSE, G. (1969): Ein Beitrag zum Problem der Erneuerung des Tiefenwassers im Arkona-Becken. Kieler Meeresf. XXV, 268—271.

KRAUSS, W. (1960): Hydrographische Messungen mit einem Beobachtungsmast in der Ostsee. Kieler Meeresf. XVI, 15—27.

KRAUSS, W. & L. MAGAARD (1962): Zum System der Eigenschwingungen der Ostsee. Kieler Meeresf. XVIII, 184—186.

KRAUSS, W. (1963): Zum Spektrum der internen Seiches der Ostsee. Kieler Meeresf. XIX, 119—132

KRAUSS, W. (1966): Interne Wellen. Gebr. Borntraeger, Berlin, 248ff.

KRAUSS, W. (1966a): Das Spektrum der internen Bewegungsvorgänge der Ostsee im Periodenbereich von 0.5—7 Stunden. Kieler Meeresf. XXII, 28—34.

KRAUSS, W. (1966b): Die Spektren der Temperaturschwankungen und der Strömung im Gebiet nordwestlich von Fehmarn. Kieler Meeresf. XXII, 35—38.

KRAUSS, W. (1972): Wind-generated internal waves and inertial-period motions. Dtsch. Hydrogr. Z. **25**, 241—250.

KRAUSS, W. (1973): Wind-driven oscillations of an enclosed basin with bottom friction. Dtsch. Hydrogr. Z. **26**, 1—9.

MAGAARD, L. & W. KRAUSS (1966): Spektren der Wasserstandsschwankungen der Ostsee im Jahre 1958. Kieler Meeresf. XXII, 155—162.

NAGATA, Y. (1964): The statistical properties of orbital wave motions and their application for the measurement of directional wave spectra. J. Oceanogr. Soc. Japan **19**, 169—181.

NEUMANN, G. (1941): Eigenschwingungen der Ostsee. Arch. Dtsch. Seewarte und Marineobserv. **61**, 4, 59 pp.

POLLARD, R. T.& R. C. MILLARD (1967): Comparison between observed and simulated wind-generated inertial oscillations. Deep-Sea Res. **17**, 813.

RAO, D. B. (1966): Free gravitational oscillations in rotating rectangular basins. J. Fluid Mech. **25**, 523—555.

SABININ, K. D. (1969): Determination of the parameters of internal waves using data from a towed chain of thermistors. Izvestiya Academy of Sciences, USSR. Atmospheric and Oceanic Physics 5, No. 2, 113—115,

SCHOTT, G. (1924): Einige Hauptergebnisse der hydrographischen Forschungen 1920—1923. Ber. Dtsch. Wiss. Komm. f. Meeresf. Neue Folge Bd. I (1919—1923, 273—292).

SCHULZ, B. (1934): Die hydrographischen Arbeiten der Deutschen Wissenschaftlichen Kommission für Meeresforschung 1930—1933. Ber. Dtsch. Wiss. Komm. f. Meeresf. Neue Folge VII, 197—212.

SCHULZ, B. (1956): Hydrographische Untersuchungen in der Ostsee 1925 bis 1938. Ergänzungsheft Reihe B (4) Nr. 1 der Dtsch. Hydrogr. Z.

SIEDLER, G. (1961): Über die kurzfristige Veränderlichkeit von Temperatur- und Salzgehaltsschichtung in der östlichen und mittleren Ostsee im Sommer 1960. Kieler Meeresf. XVII, 148—153.

STARR, V. P. (1968): Physics of negative viscosity Phenomena. Mc Graw Hill, New York, 256 pp.

TOMCZAK, M. jr. (1966): Winderzeugte interne Wellen, insbesondere im Periodenbereich oberhalb der Trägheitsperiode. Dt. Hydrogr. Z. **19**, 1, 1—21.

TOMCZAK, M. jr. (1967): Über den Einfluß fluktuierender Windfelder auf ein stetig geschichtetes Meer. Dt. hydrogr. Z. **20**, 101—129.

Tomczak, M. jr. (1969): Über interne Trägheitsbewegungen in der westlichen Ostsee. Dt. Hydrogr. Z. **22**, 4, 158—162.

WALIN, G. (1972): On the hydrographic response to transient meteorological disturbances. Tellus XXIV, 169—186.

WATTENBERG, H. (1949): Die Salzgehaltsverteilung in der Kieler Bucht und ihre Abhängigkeit von Strom- und Wetterlage. Kieler Meeresf. VI, 17—30.

WEBSTER, F. (1967): A scheme for sampling deep-sea currents from moored buoys. Trans. 2nd Int. Buoy Techn. Symp., Marine Techn. Soc. Washington, 419—431.

WEBSTER, F. (1968): Observations of inertial-period motions in the deep sea. Rev. Geoph. **5**, 473.

WEIDEMANN, H. (1950): Untersuchungen über unperiodische und periodische hydrographische Vorgänge in der Beltsee. Kieler Meeresf. VII, 70—86.

WITTIG, H. (1953): Der mittlere jährliche Gang des Salzgehaltes in der Kieler und Mecklenburger Bucht, Kieler Meeresf. IX, 2, 171—175.

WYRTKI, K. (1953, 1954): Die Dynamik der Wasserbewegungen im Fehmarnbelt I und II. Kieler Meeresf. IX, 155—170 und X, 162—181.